

A Comparison of RANS, URANS, and DDES for High-Lift Systems from HiLiftPW-3

Riccardo Balin and Kenneth E. Jansen

Ann and H. J. Smead Department of Aerospace Engineering Sciences
University of Colorado - Boulder

AIAA SciTech Forum
January 10th, 2018



Ann and H.J. Smead Aerospace Engineering
UNIVERSITY OF COLORADO BOULDER

Outline

- Overview of cases studied and numerical computations
- Numerical results
 - Grid convergence study on HL-CRM model
 - Effects of initial conditions JSM
 - RANS, URANS, and DDES on JSM
- Conclusions



Workshop Cases Studied

HL-CRM

Cases	Angles of Attack (AoA)	Notes
1a	8°, 16°	<ul style="list-style-type: none">grid refinement studyfull-gap geometryB1 committee grids, Coarse-Medium-Fine
1b	16°	<ul style="list-style-type: none">grid adaptation studyfull-gap geometryin-house, Simmetrix grids

JSM

Cases	Angles of Attack (AoA)	Notes
2a	4.36°, 10.47°, 14.54°, 18.58°, 20.59°, 21.57°	<ul style="list-style-type: none">no nacelleC1 committee grid, M
2b	21.57°	<ul style="list-style-type: none">no nacelleDDESadaptation study, in-house Simmetrix grids
2c	4.36°, 10.47°, 14.54°, 18.58°, 20.59°, 21.57°	<ul style="list-style-type: none">with nacelleC1 committee grid, M



Workshop Cases Studied

HL-CRM

Cases	Angles of Attack (AoA)	Notes
1a	8°, 16°	<ul style="list-style-type: none"> grid refinement study full-gap geometry B1 committee grids, Coarse-Medium-Fine
1b	16°	<ul style="list-style-type: none"> grid adaptation study full-gap geometry in-house, Simmetrix grids <div>in progress</div>

JSM

Cases	Angles of Attack (AoA)	Notes
2a	4.36°, 10.47°, 14.54°, 18.58°, 20.59°, 21.57°	<ul style="list-style-type: none"> no nacelle C1 committee grid, M
2b	21.57°	<ul style="list-style-type: none"> no nacelle DDES adaptation study, in-house Simmetrix grids <div>in progress</div>
2c	4.36°, 10.47°, 14.54°, 18.58°, 20.59°, 21.57°	<ul style="list-style-type: none"> with nacelle C1 committee grid, M



Workshop Cases Studied

HL-CRM

Cases	Angles of Attack (AoA)	Notes
1a	8°, 16°	<ul style="list-style-type: none"> grid refinement study full-gap geometry B1 committee grids, Coarse-Medium-Fine
1b	16°	<ul style="list-style-type: none"> grid adaptation study full-gap geometry in-house, Simmetrix grids <div>in progress</div>

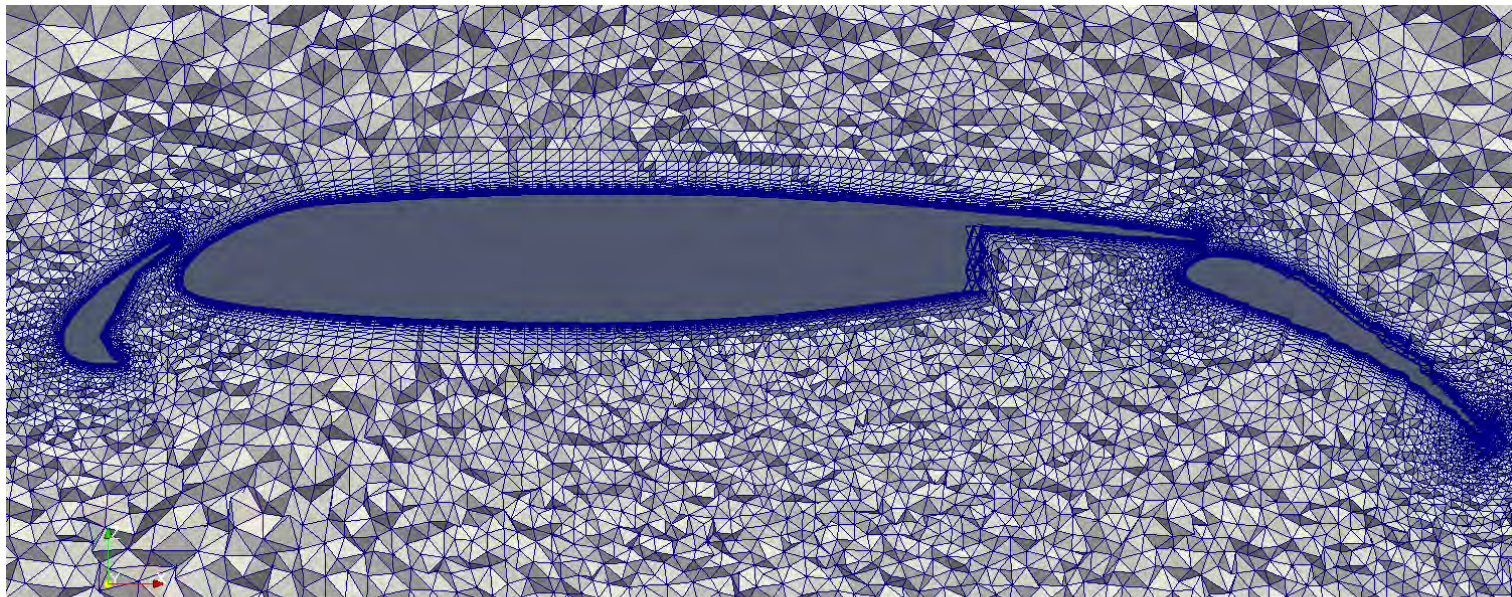
JSM

Cases	Angles of Attack (AoA)	Notes
2a	4.36°, 10.47°, 14.54°, 18.58°, 20.59°, 21.57°	<ul style="list-style-type: none"> no nacelle C1 committee grid, M
2b	21.57°	<ul style="list-style-type: none"> no nacelle DDES adaptation study, in-house Simmetrix grids <div>in progress</div>
2c	4.36°, 10.47°, 14.54°, 18.58°, 20.59°, 21.57°	<ul style="list-style-type: none"> with nacelle C1 committee grid, M



Numerical Set-Up

- Computations carried out with PHASTA stabilized, finite element flow solver.
- Spalart-Allmaras (SA) one-equation model (QCR results run, not focus here).
- All computations run fully turbulent, no specified transition.
- Incompressible Navier-Stokes equations solved.
- All results are with global time stepping: will cite time step in chord flights.



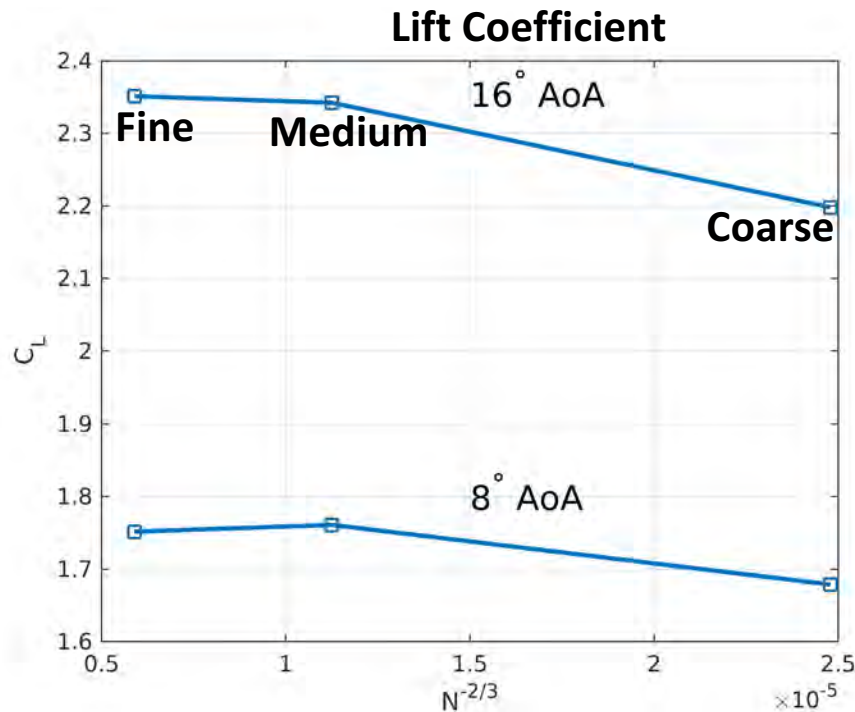
Slice across wing section of the JSM grid used



HL-CRM – Grid Convergence Study

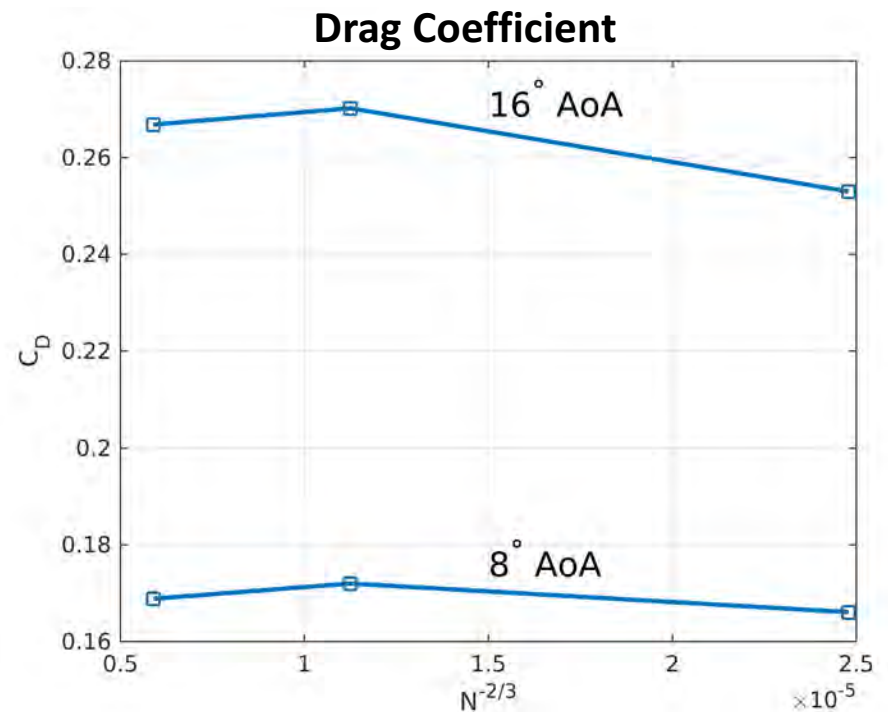
Lift:

- About 5% under-prediction with Coarse
- Medium within 1% of Fine for both AoA
- Medium converged to “true” solution



Drag:

- Slower convergence, Med. grid not within 1% of Fine

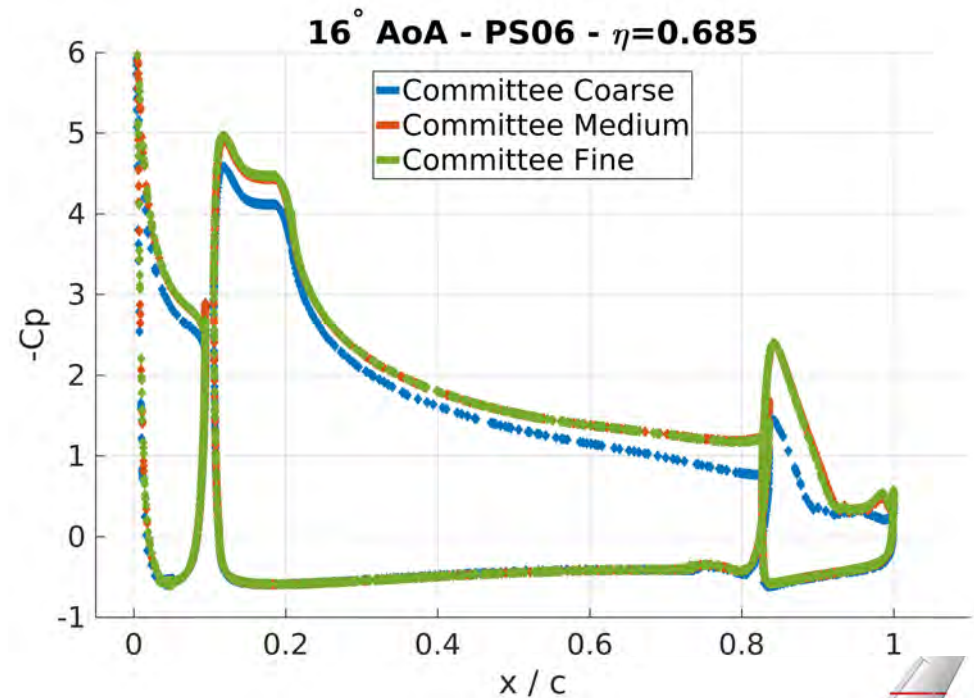
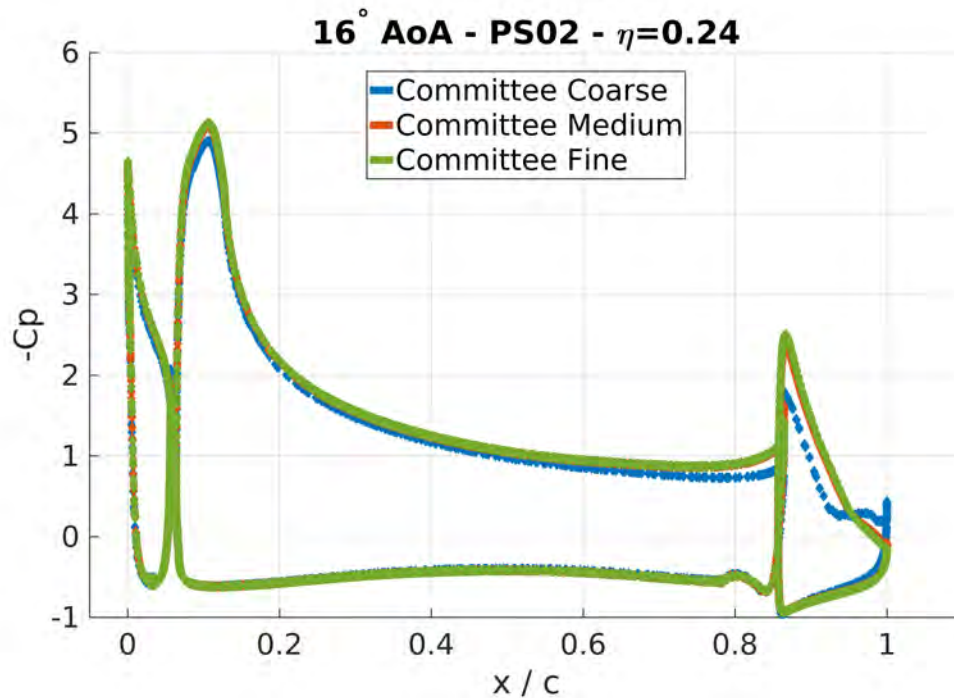


Lift and drag coefficients vs. number of grid points to -2/3 power

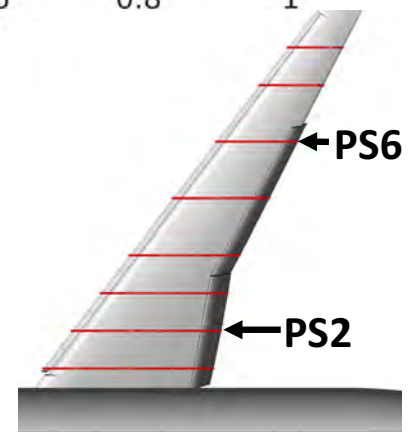


HL-CRM – Grid Convergence Study

Pressure coefficient profiles at 24% and 68% of the half-span for 16° AoA



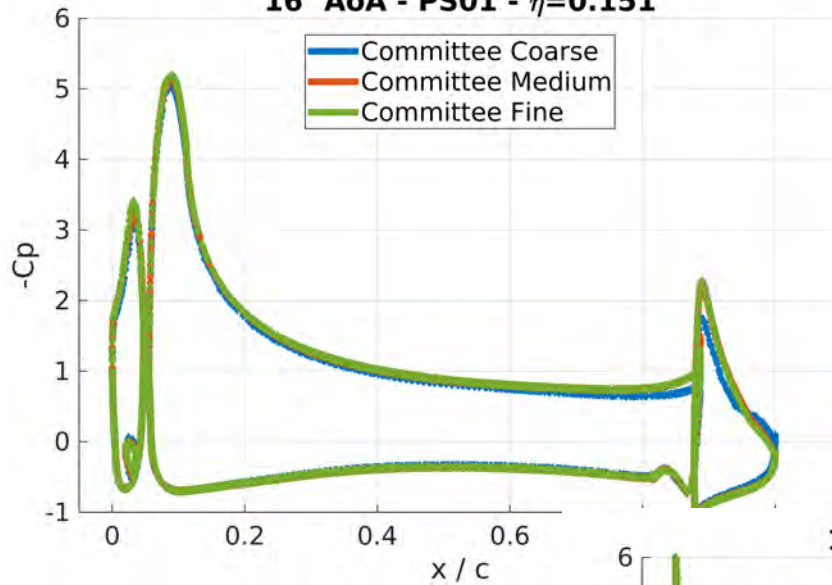
- Excessive flow separation over both flaps with Coarse grid
- Medium and Fine grids almost identical.



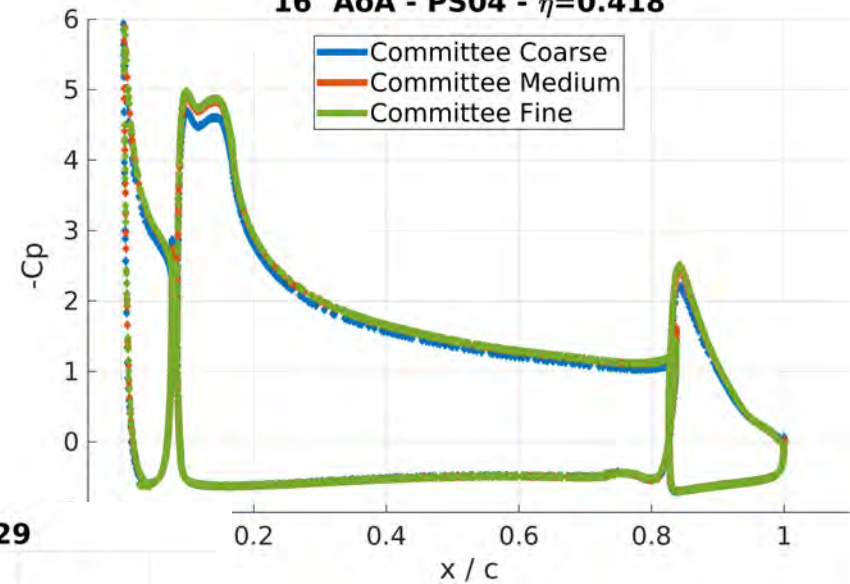
HL-CRM – Grid Convergence Study

Pressure coefficient profiles at other pressure stations for 16° AoA

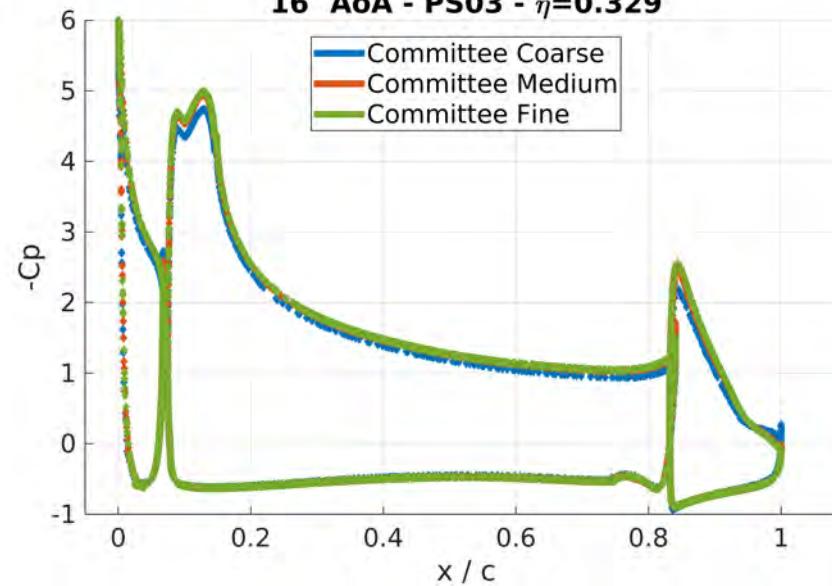
16° AoA - PS01 - $\eta=0.151$



16° AoA - PS04 - $\eta=0.418$



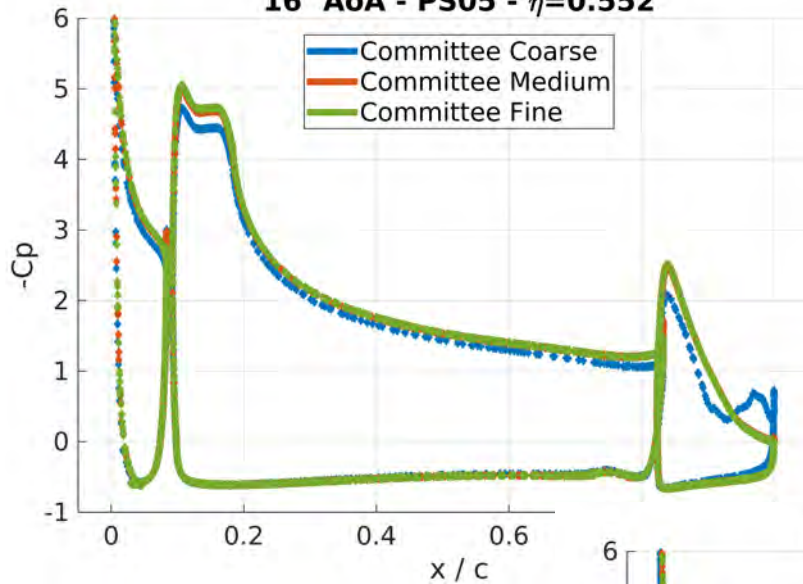
16° AoA - PS03 - $\eta=0.329$



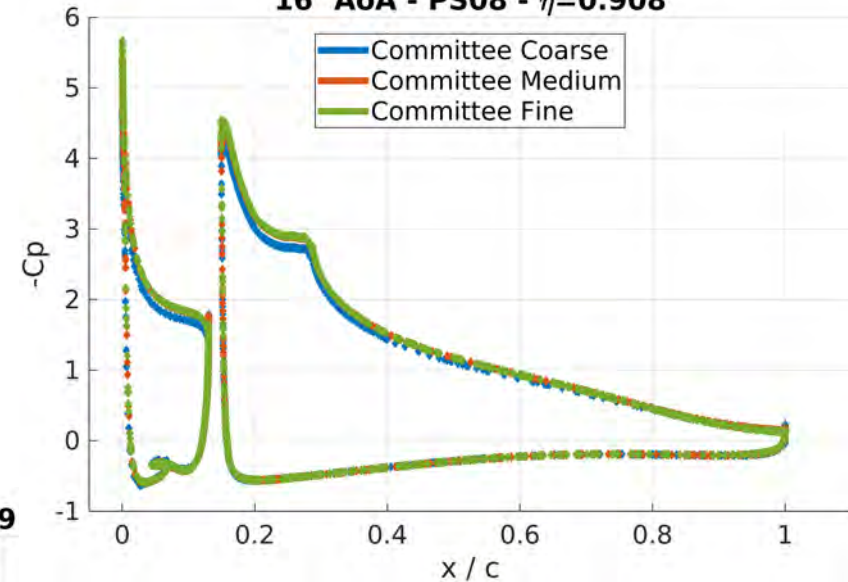
HL-CRM – Grid Convergence Study

Pressure coefficient profiles at other pressure stations for 16° AoA

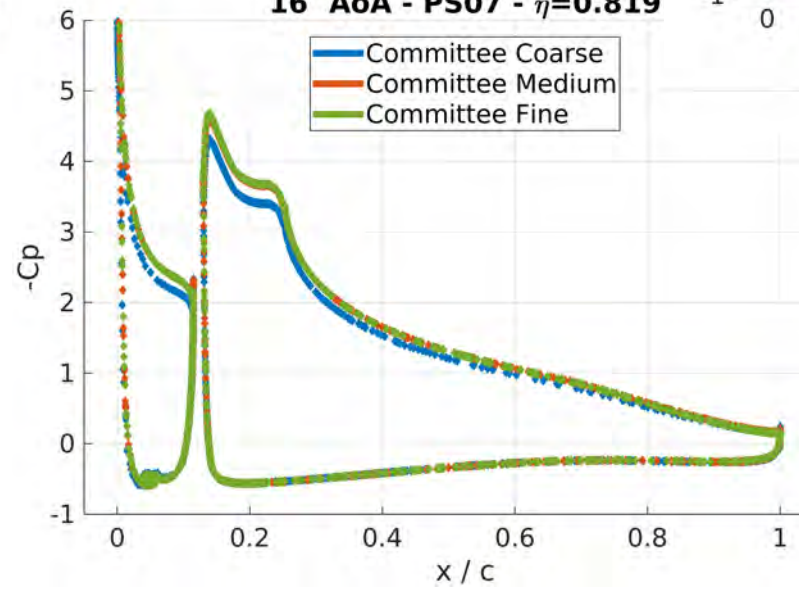
16° AoA - PS05 - $\eta=0.552$



16° AoA - PS08 - $\eta=0.908$

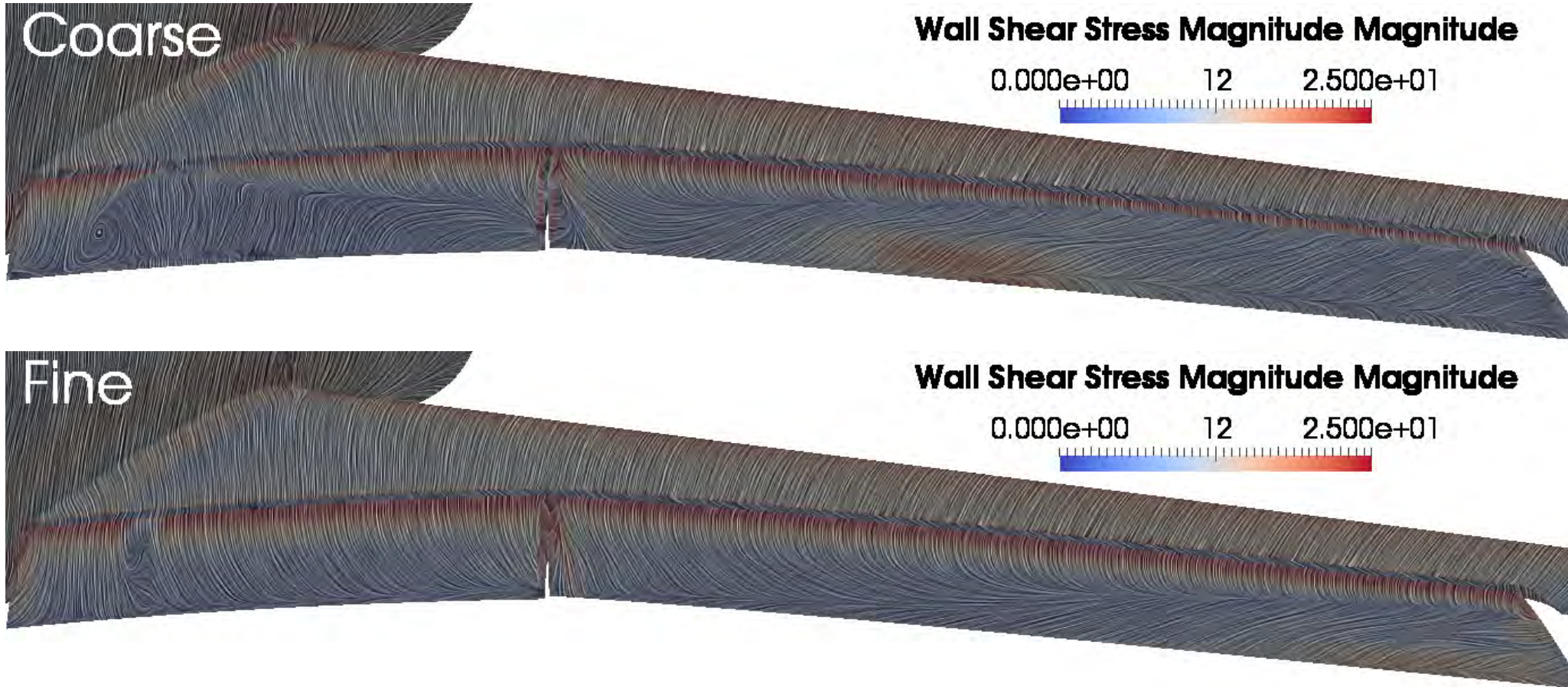


16° AoA - PS07 - $\eta=0.819$



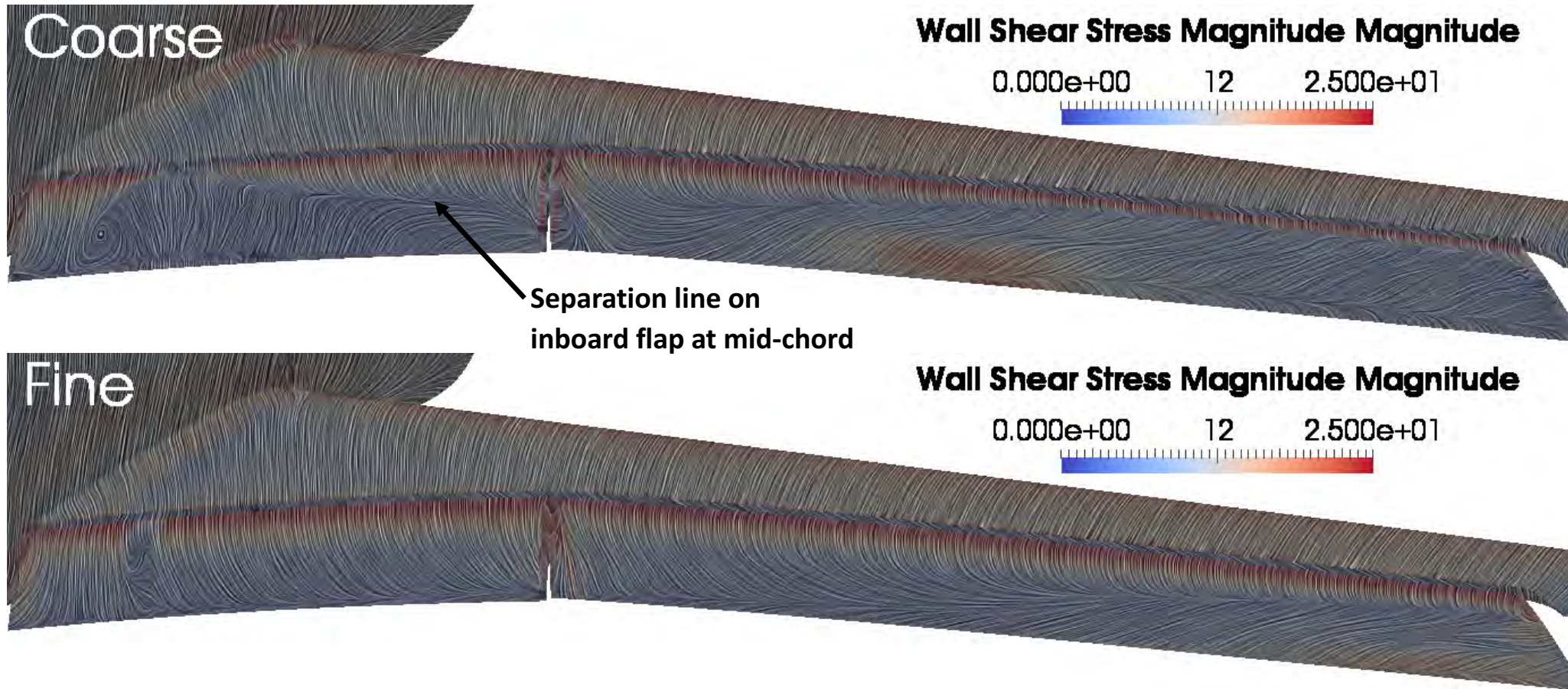
HL-CRM – Grid Convergence Study

Surface Line Integral Convolution of Wall Shear Stress at 16° AoA



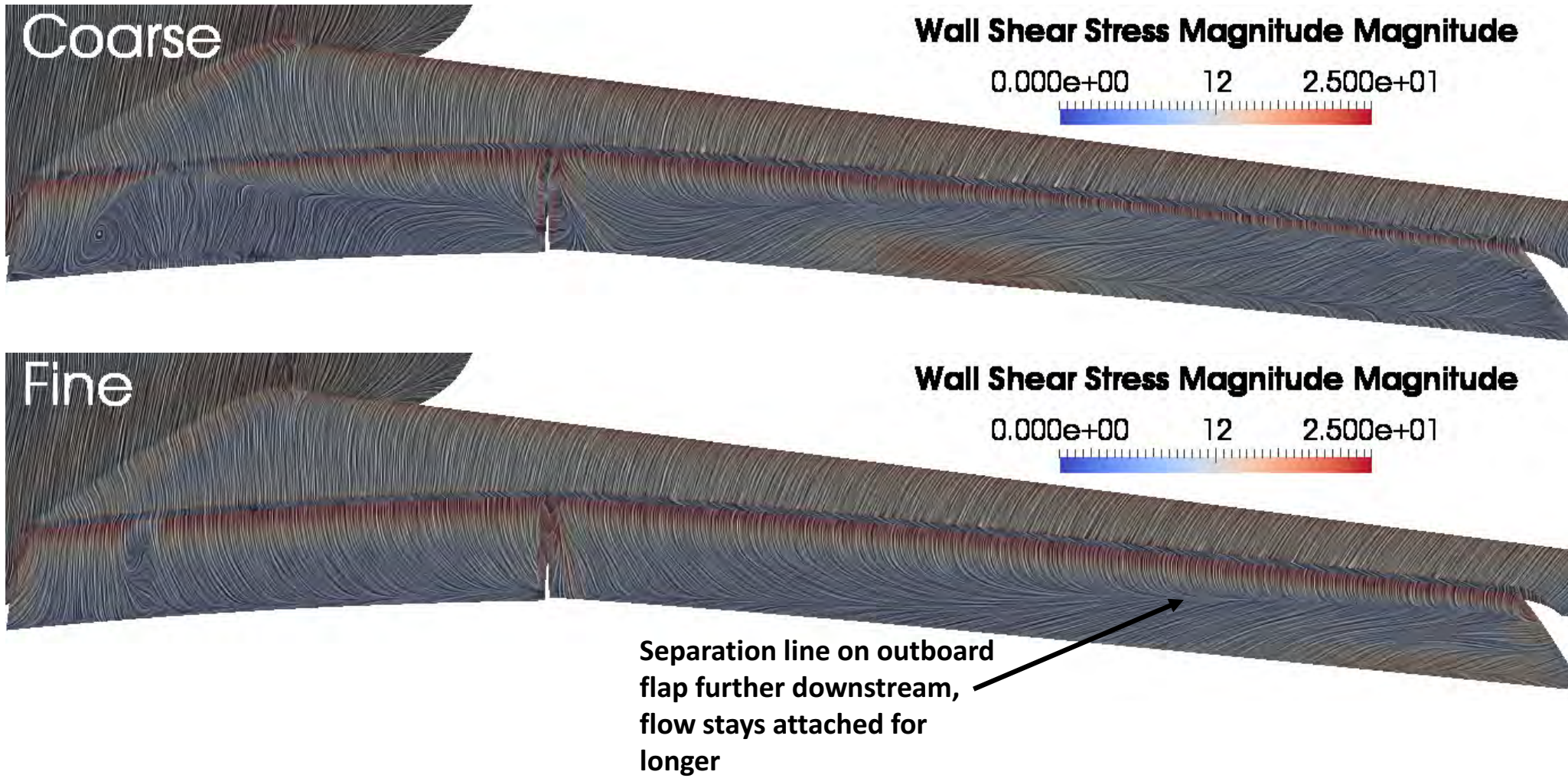
HL-CRM – Grid Convergence Study

Surface Line Integral Convolution of Wall Shear Stress at 16° AoA



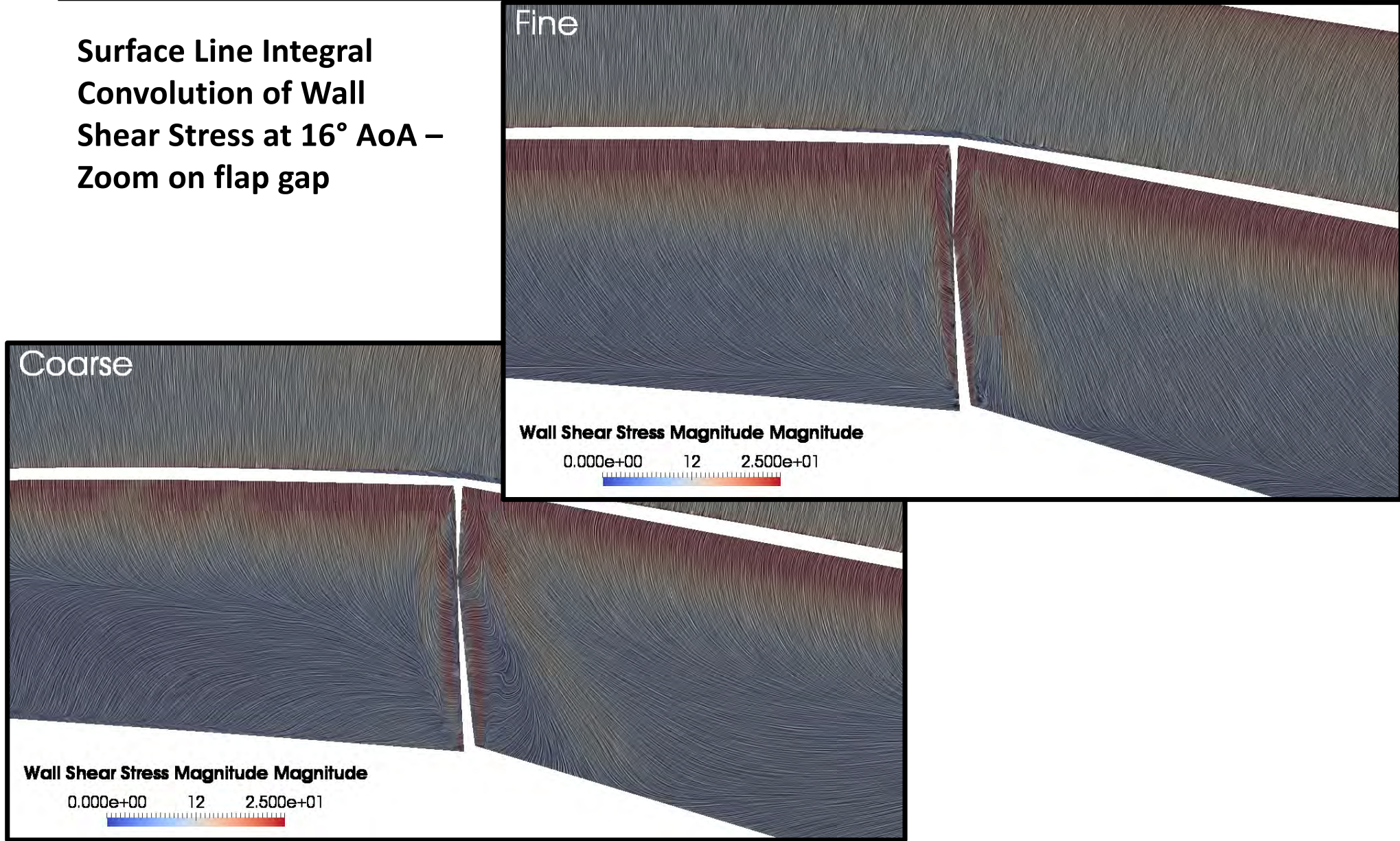
HL-CRM – Grid Convergence Study

Surface Line Integral Convolution of Wall Shear Stress at 16° AoA



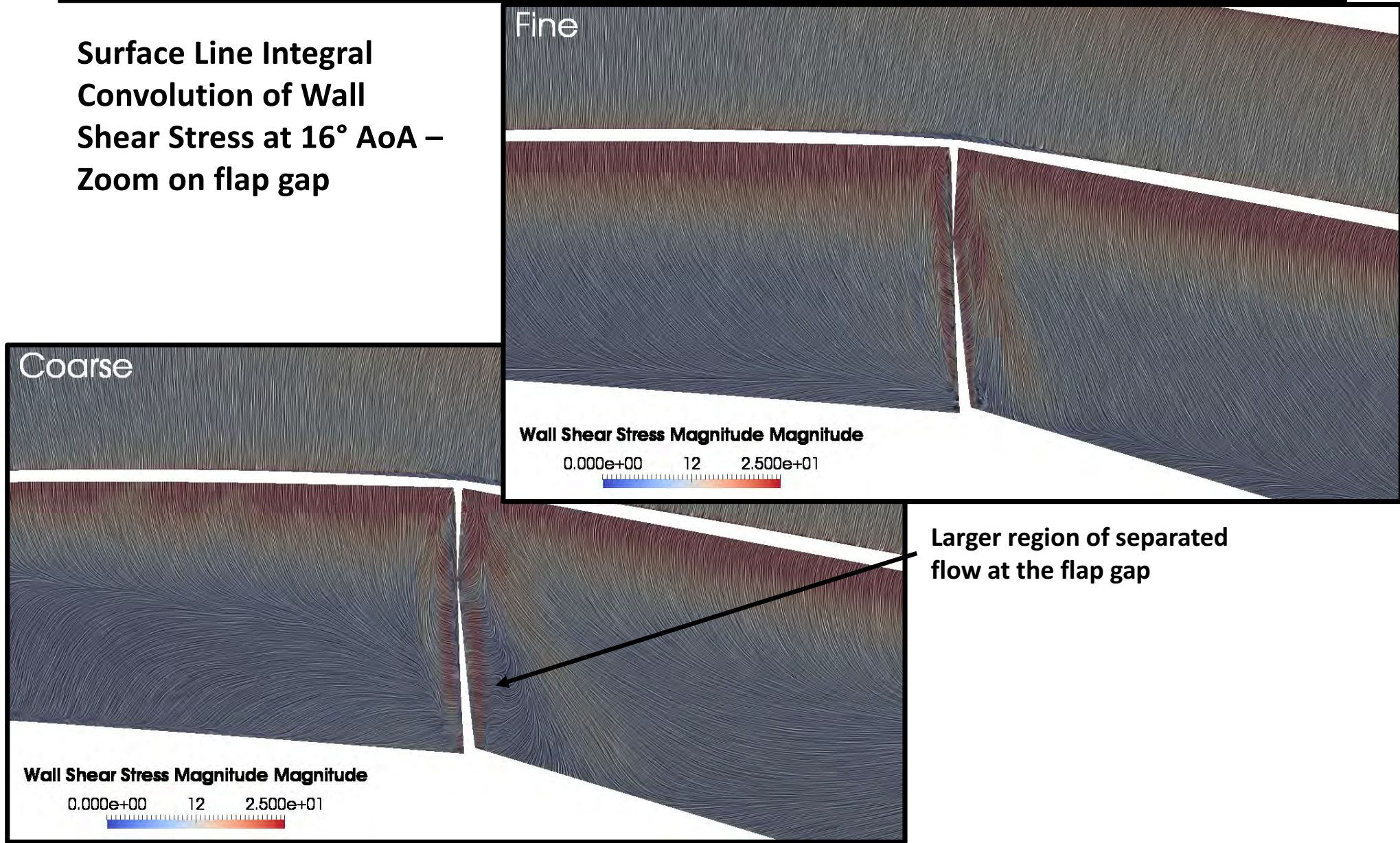
HL-CRM – Grid Convergence Study

Surface Line Integral
Convolution of Wall
Shear Stress at 16° AoA –
Zoom on flap gap



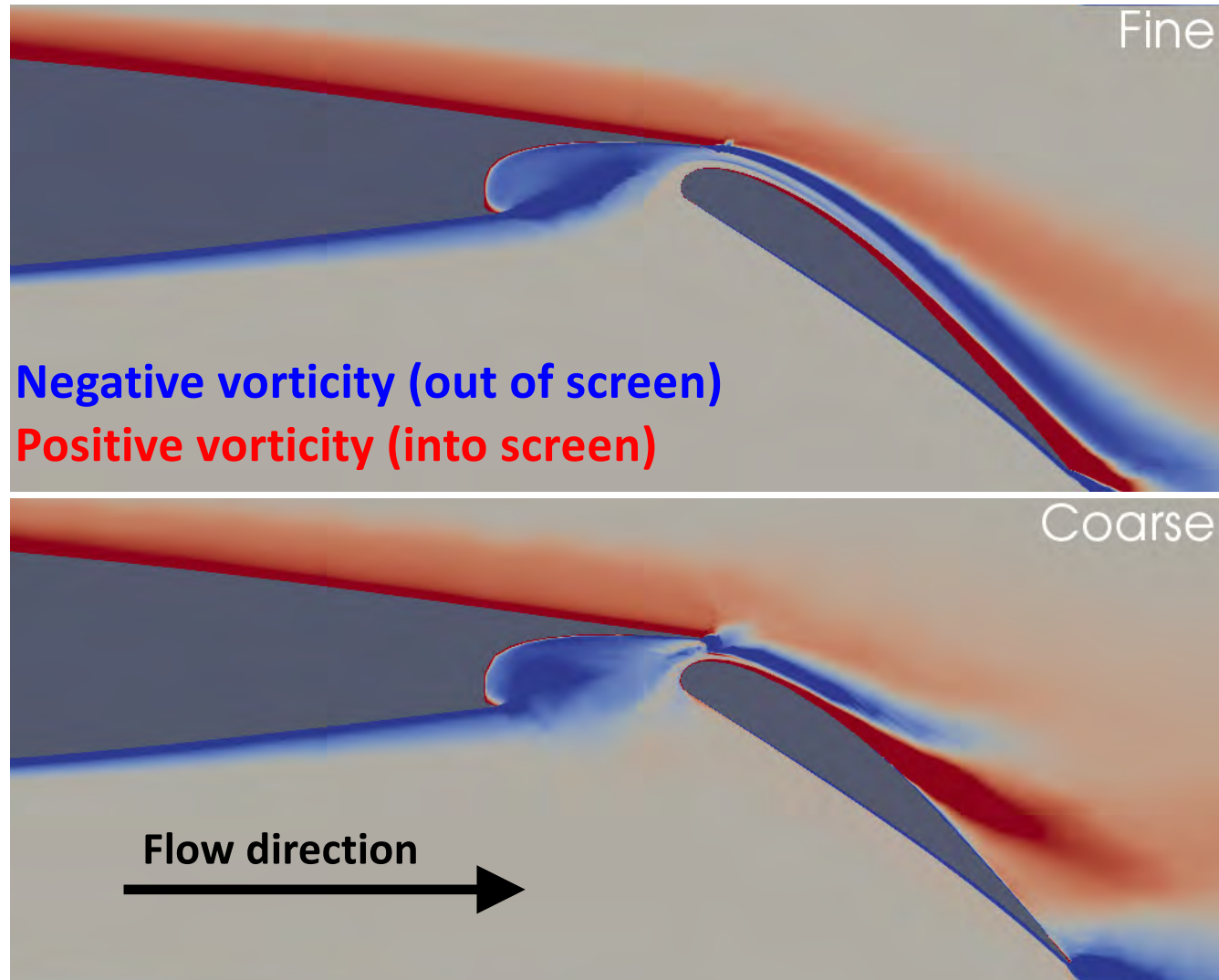
HL-CRM – Grid Convergence Study

Surface Line Integral
Convolution of Wall
Shear Stress at 16° AoA –
Zoom on flap gap



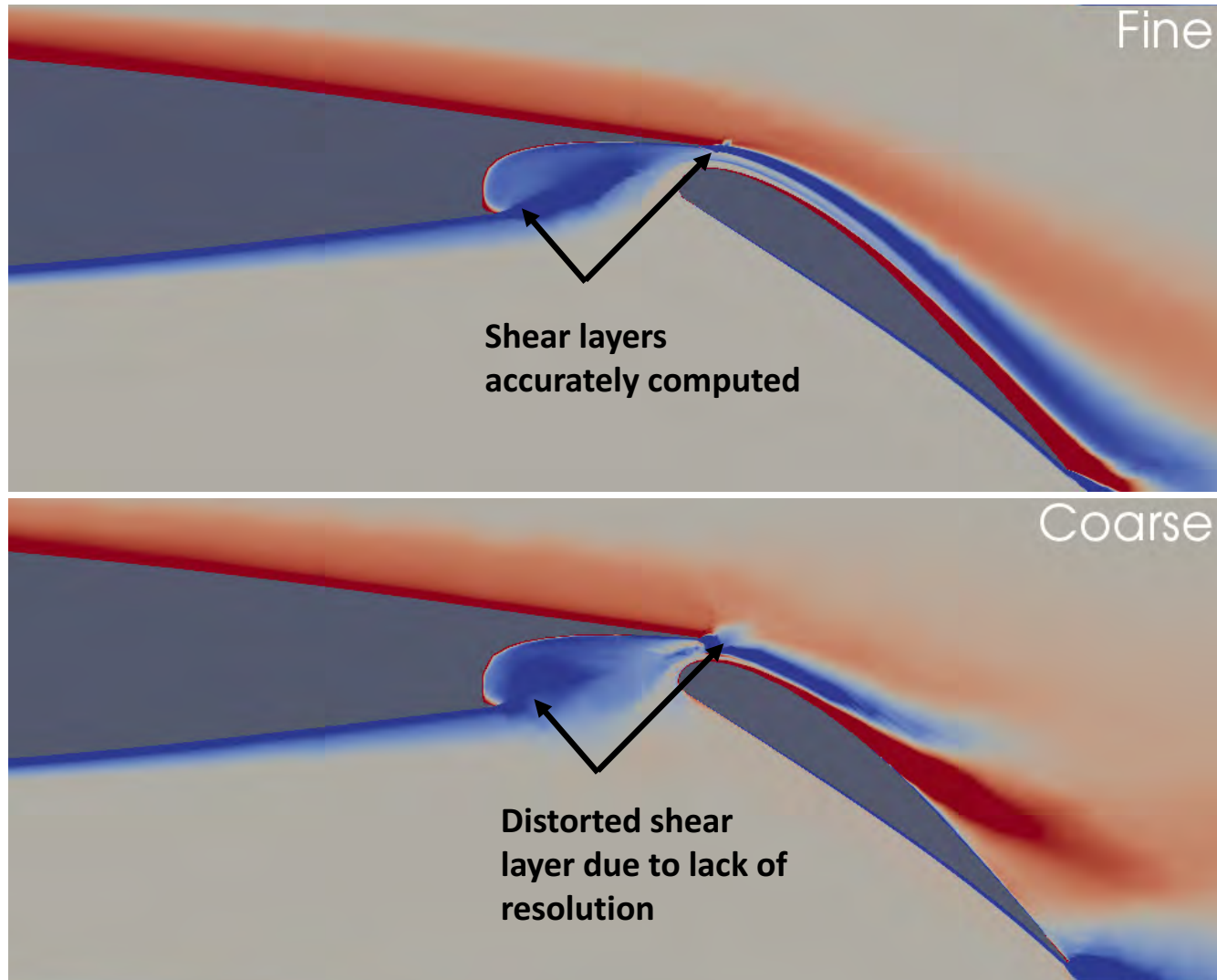
HL-CRM – Grid Convergence Study

Slice at 24% of half-span colored by span-wise vorticity



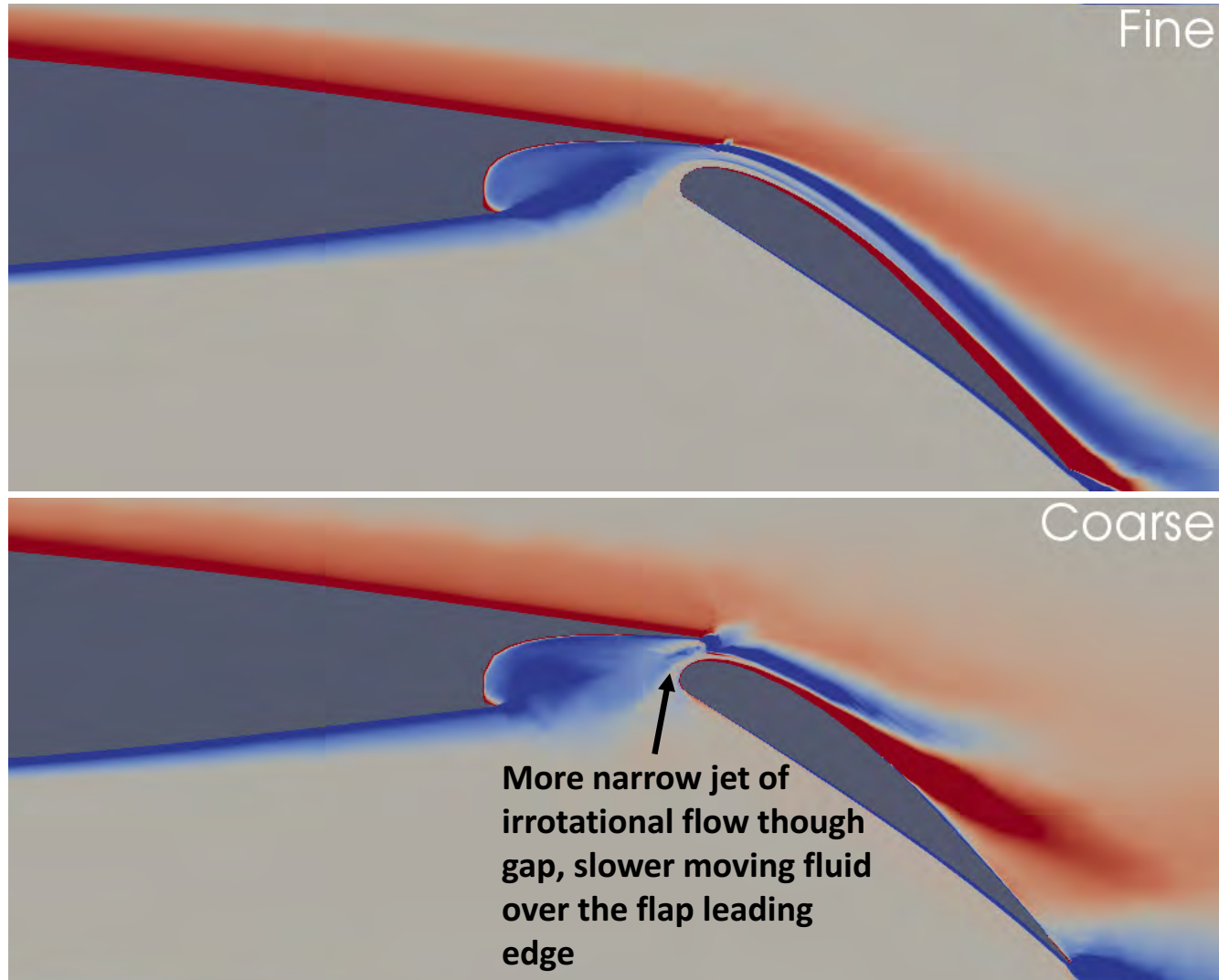
HL-CRM – Grid Convergence Study

Slice at 24% of half-span colored by span-wise vorticity



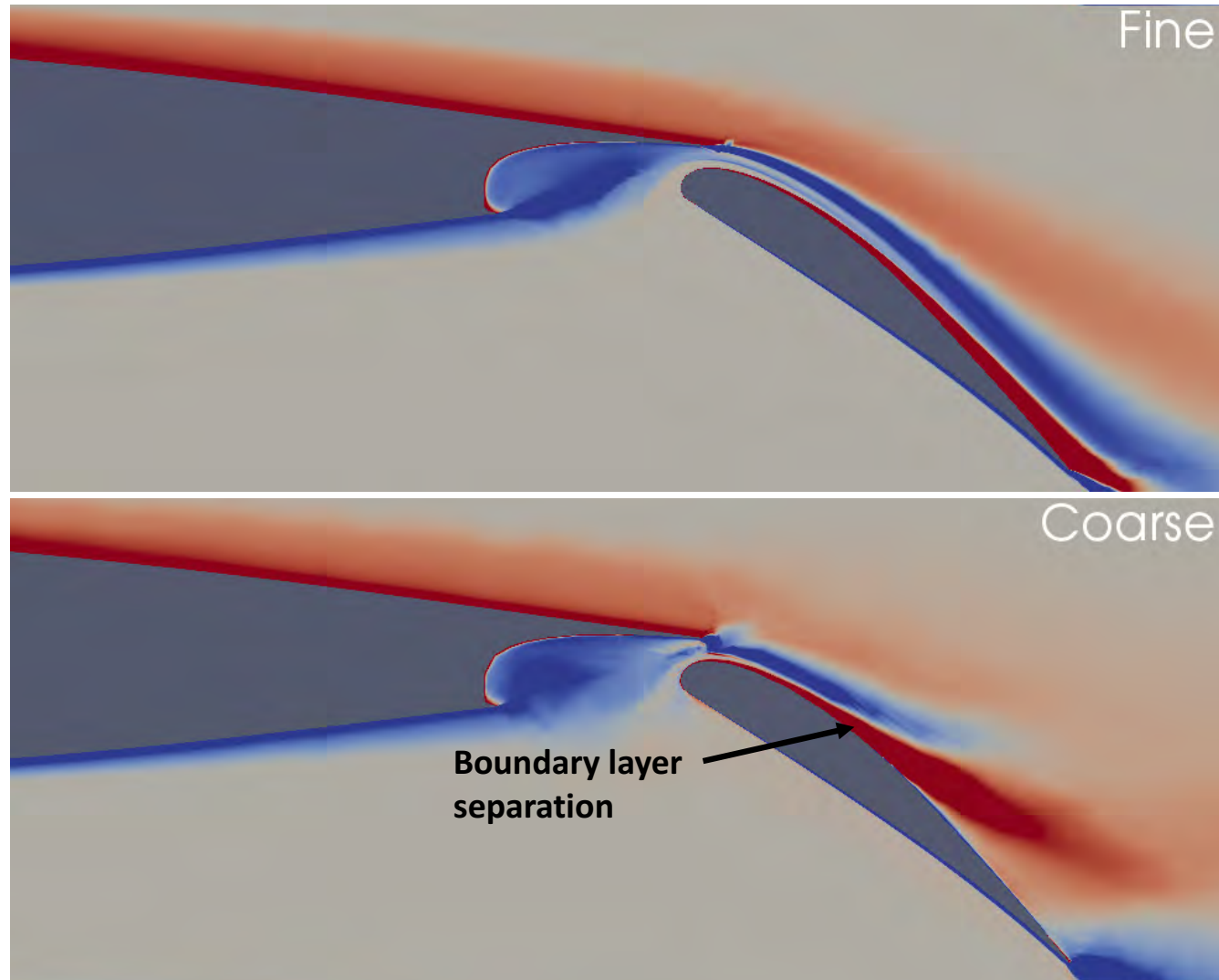
HL-CRM – Grid Convergence Study

Slice at 24% of half-span colored by span-wise vorticity



HL-CRM – Grid Convergence Study

Slice at 24% of half-span colored by span-wise vorticity



HL-CRM – Grid Convergence Study

Interim summary:

- Medium grid sufficient for convergence to within 1% for lift, slightly more than 1% for drag.
- Coarse grid has excessive separation over the flaps.
- Cause of excessive separation is the poor resolution of the flap cove shear layer separation, the main element wake, and the flap gap.

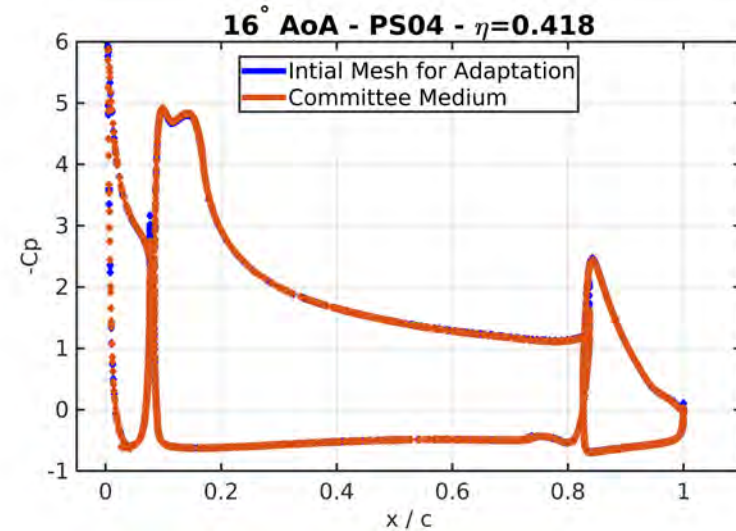
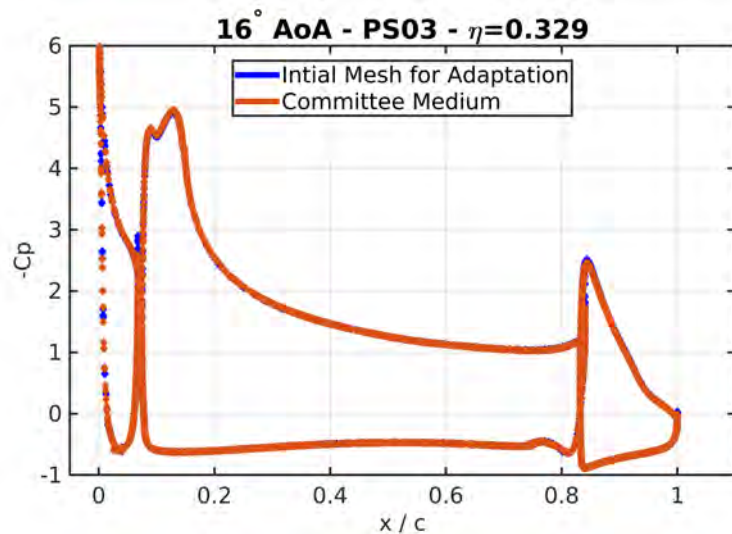
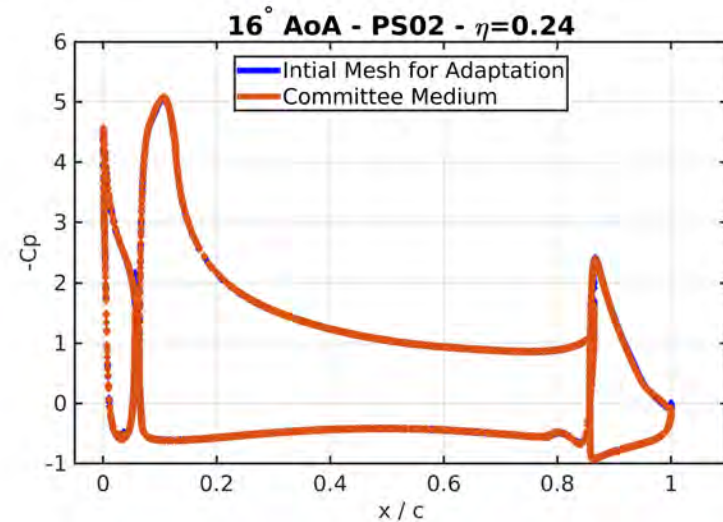
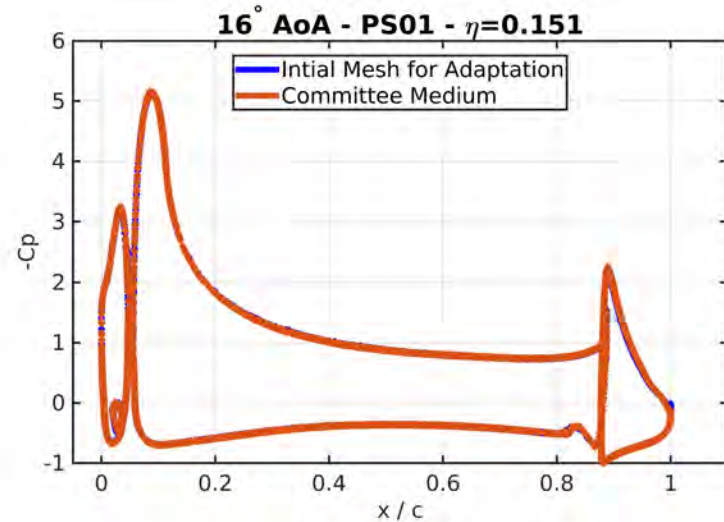
Adaptivity:

- This case poses a difficult challenge for adaptivity: Medium grid only 3x larger gives close to fine solution leaves narrow margin for adaptive “win”. Fine grid only 9x larger.
- In our experience, fully automatic anisotropic adaptivity can require 4 or more cycles of adaptation and result in grids as large as medium. Worthwhile?
- We explored a simpler approach:
 - Start adaptation from a grid that uses Coarse “surface” grid with selected improvement in gaps and Medium normal spacing, growth, and trailing edge thickness (new mesh is 14.5M nodes vs {8,26.5,70} M for {C,M,F}),
 - Attempt, in one adaptation, to improve locations of surface grid inadequacy to the same level as fine.
 - Goal: yield same quality as fine for less computational effort than medium.



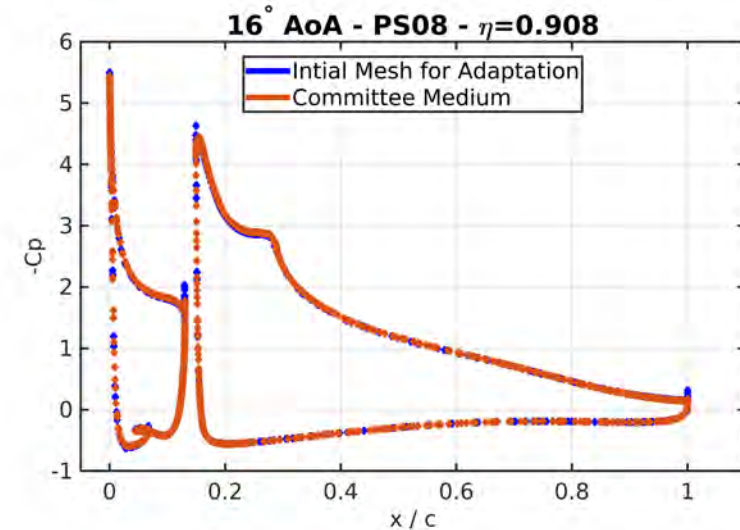
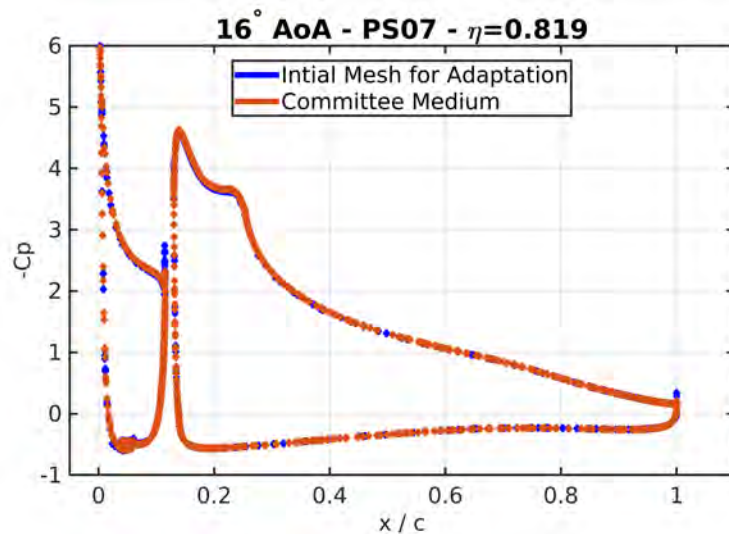
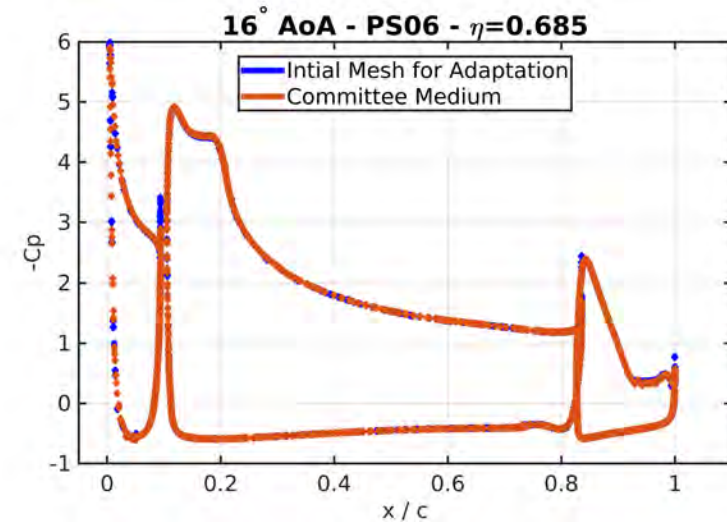
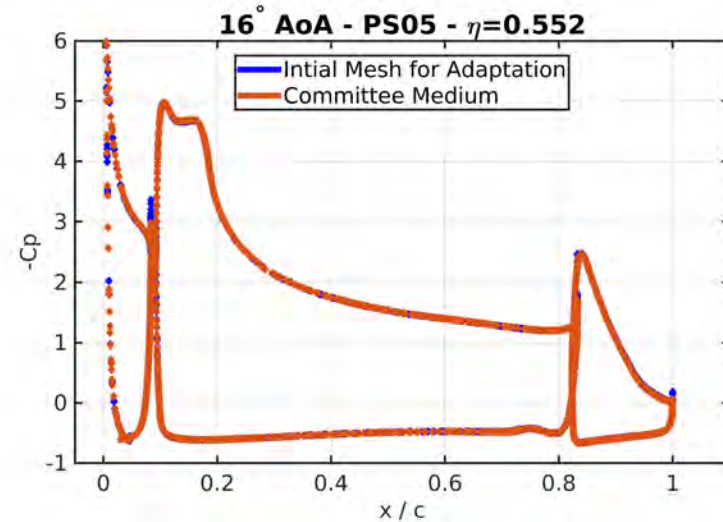
HL-CRM – Custom Grid for Adaptivity

Pressure coefficient profiles at inboard pressure stations for 16° AoA



HL-CRM – Custom Grid for Adaptivity

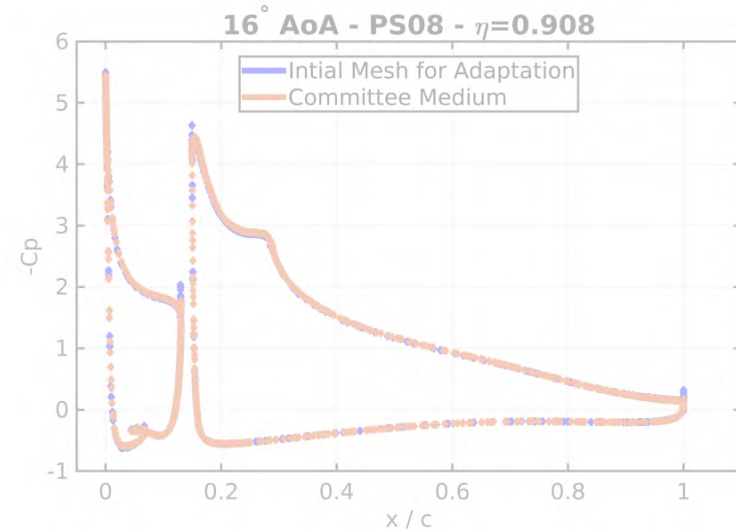
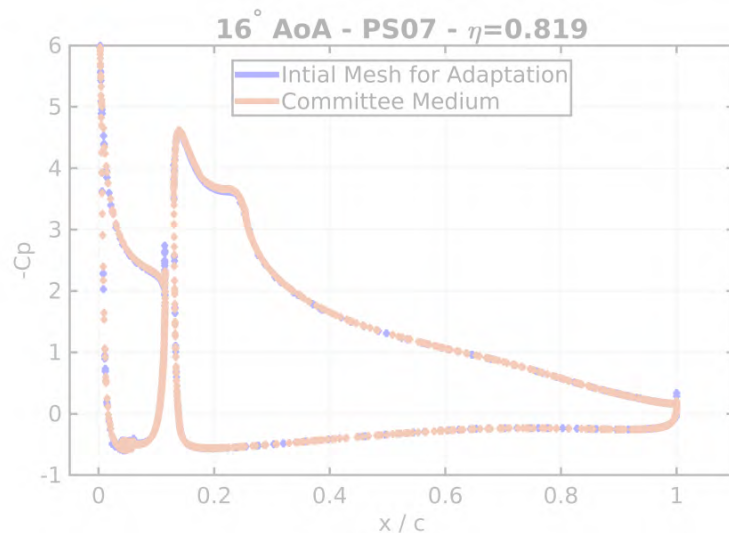
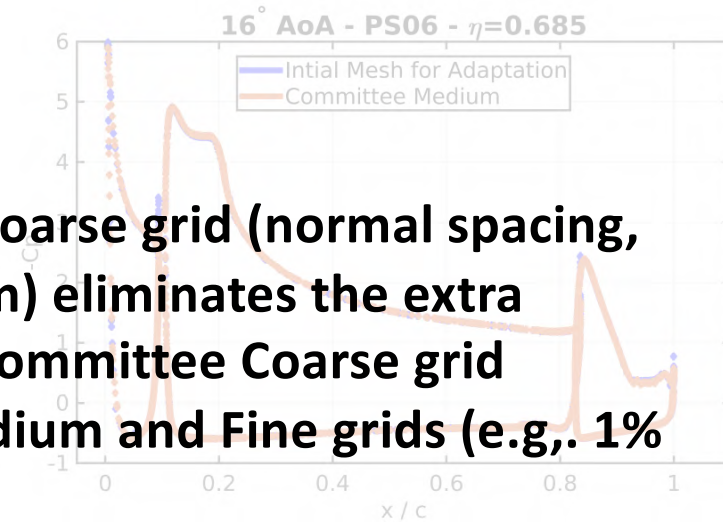
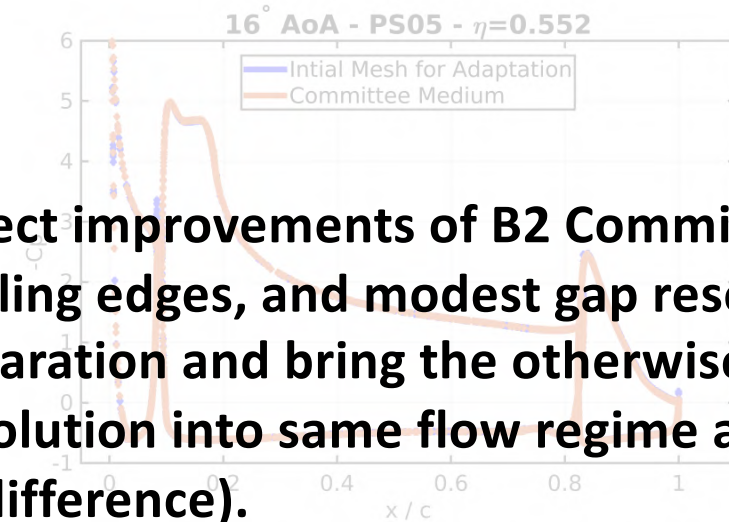
Pressure coefficient profiles at outboard pressure stations for 16° AoA



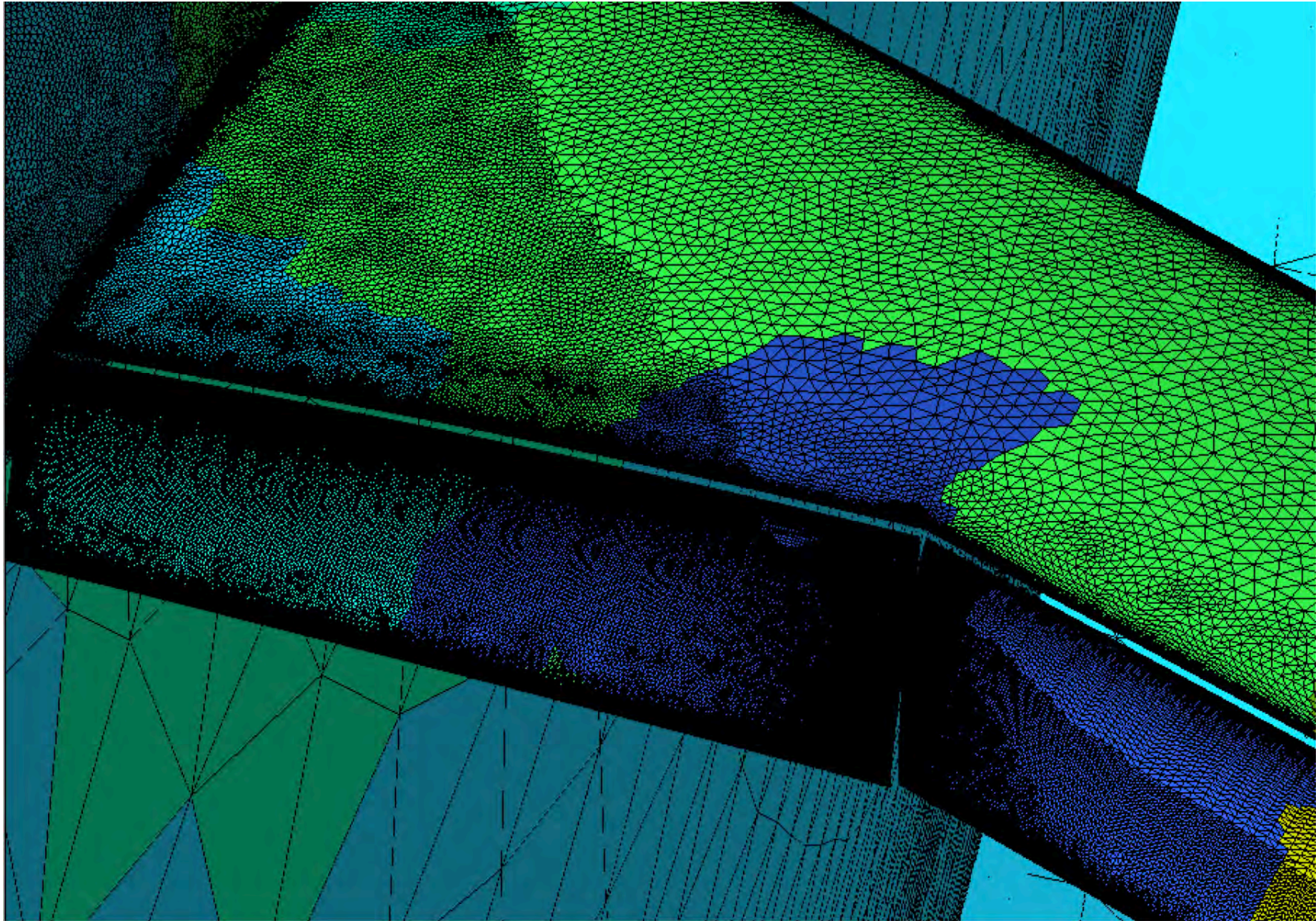
HL-CRM – Custom Grid for Adaptivity

Pressure coefficient profiles at outboard pressure stations for 16° AoA

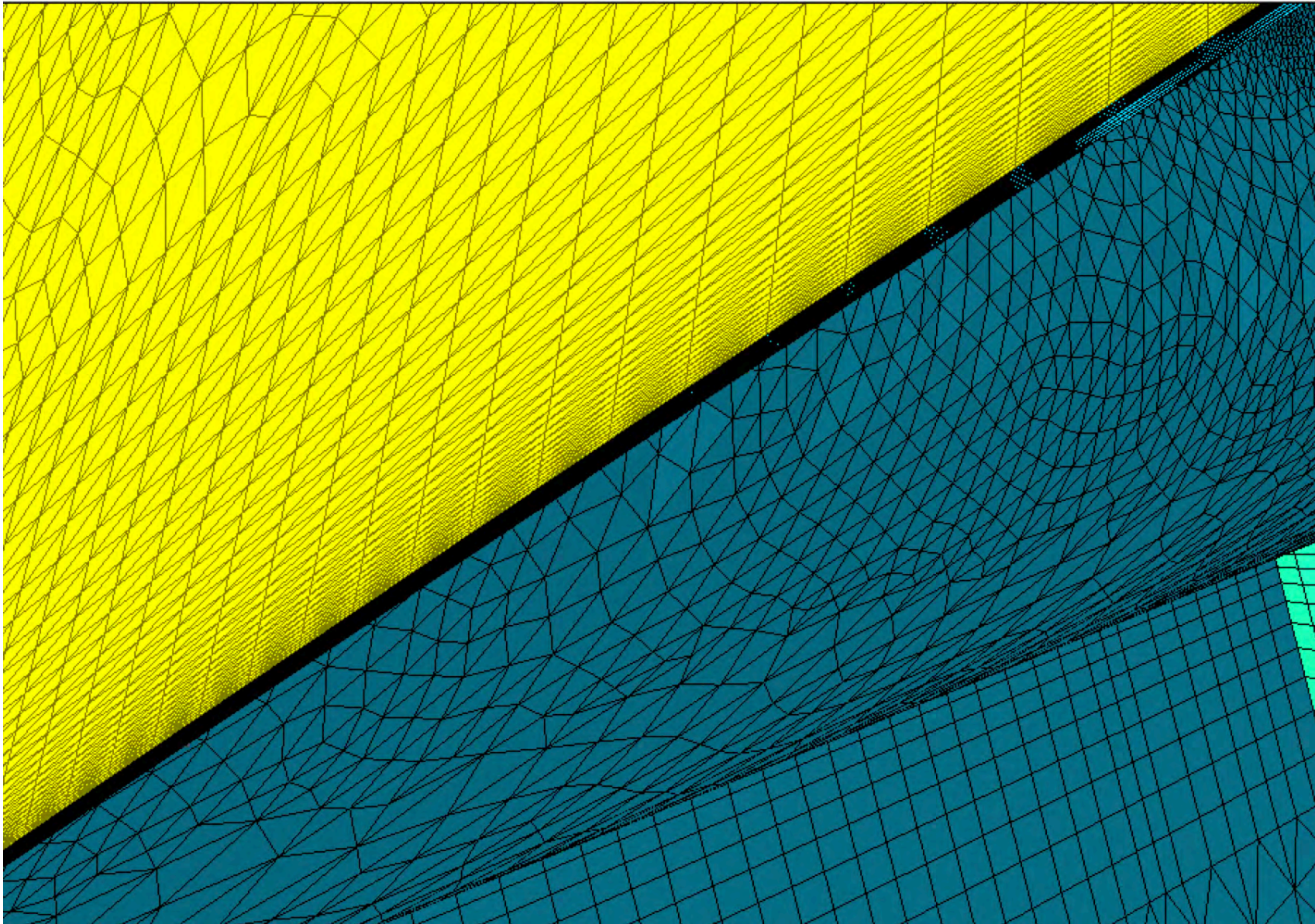
Select improvements of B2 Committee Coarse grid (normal spacing, trailing edges, and modest gap resolution) eliminates the extra separation and bring the otherwise B2 Committee Coarse grid resolution into same flow regime as Medium and Fine grids (e.g., 1% C_L difference).



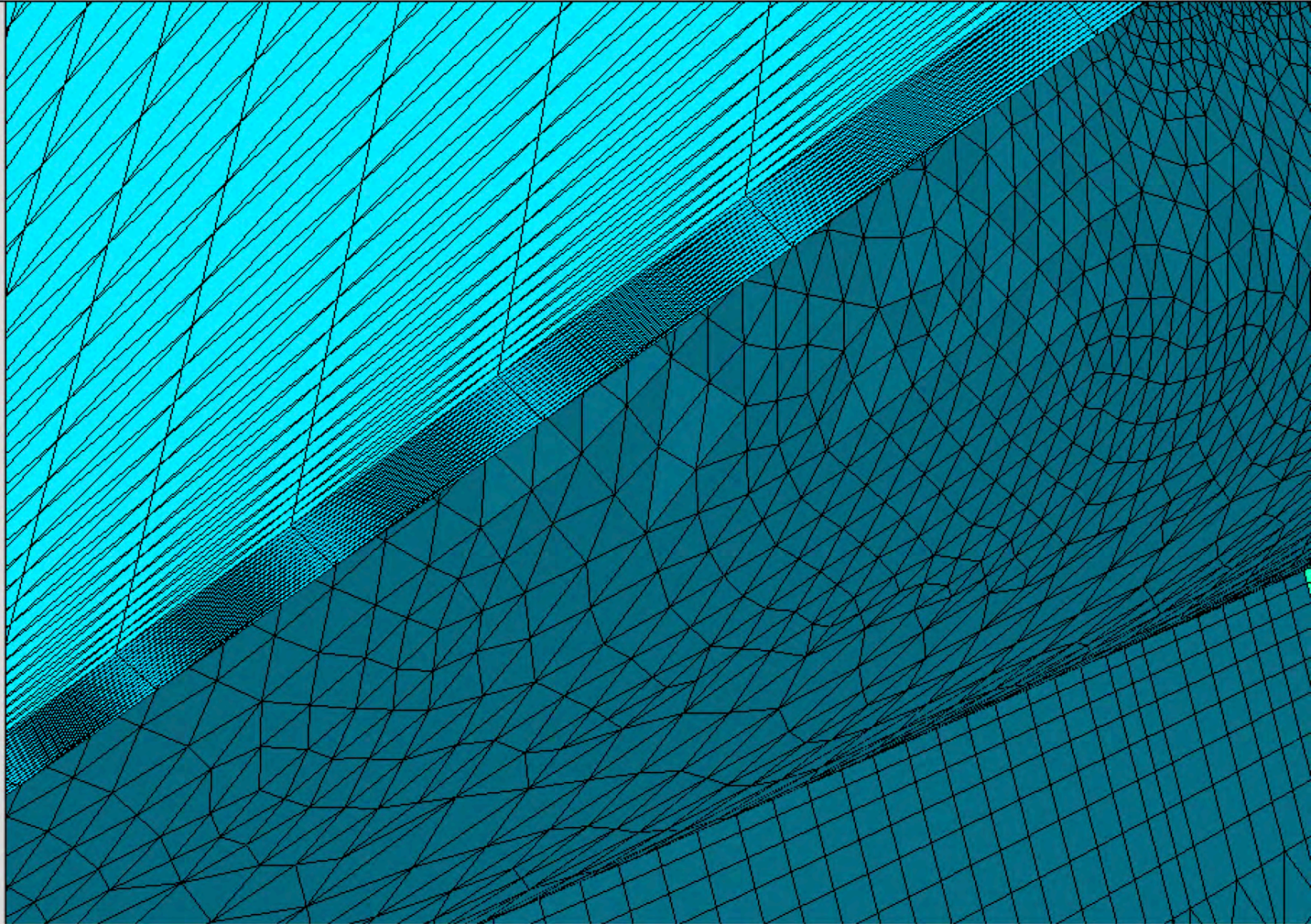
Preliminary Adaptivity



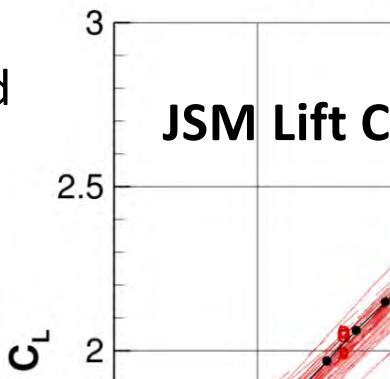
Preliminary Adaptivity: Preserve Surface Anisotropy

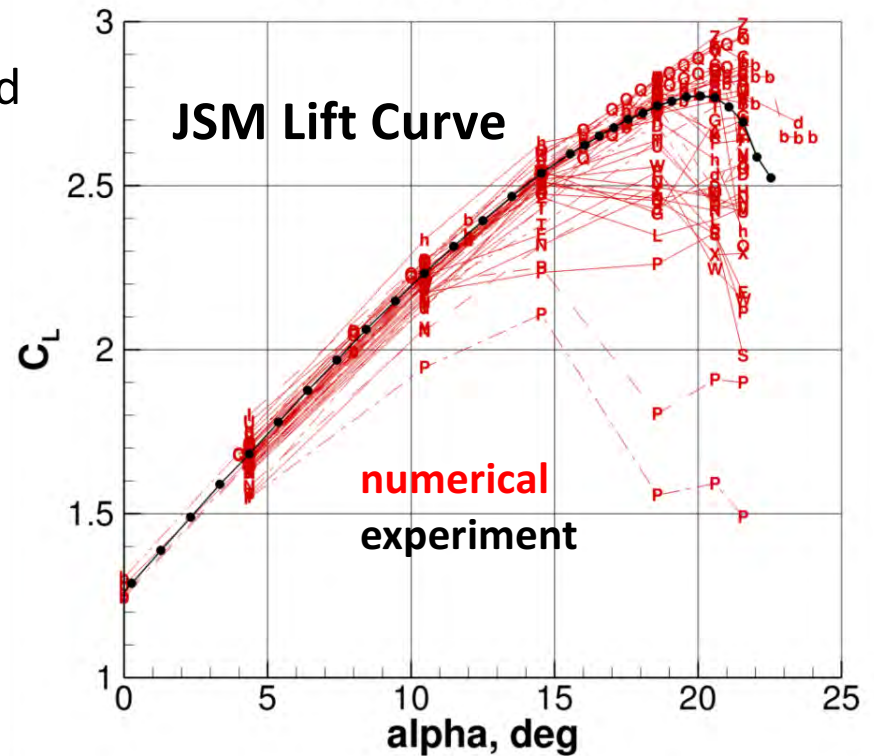


Adaptivity: Fine Grid Resolution Only Where Required



JSM – Effects of Initial Conditions

- Significant variation in participant predictions due to:
 - Flow solver (numerics)
 - Turbulence model
 - Modeling strategy (initial conditions (IC), time step size, etc.)
 - Grids
 - Most groups used steady RANS, but observed two main strategies for initial conditions
 - Starting every angle of attack from free stream conditions
 - Using converged solution at smaller angle of attack – alpha continuation
- 
- A scatter plot showing the relationship between the angle of attack α (x-axis, ranging from 0 to 10) and the JSM Lift Coefficient C_L (y-axis, ranging from 2 to 3). The plot displays several data series, likely representing different computational models or experimental results, showing a positive correlation between α and C_L . The data points are clustered around a diagonal line, indicating a consistent trend across the different models.

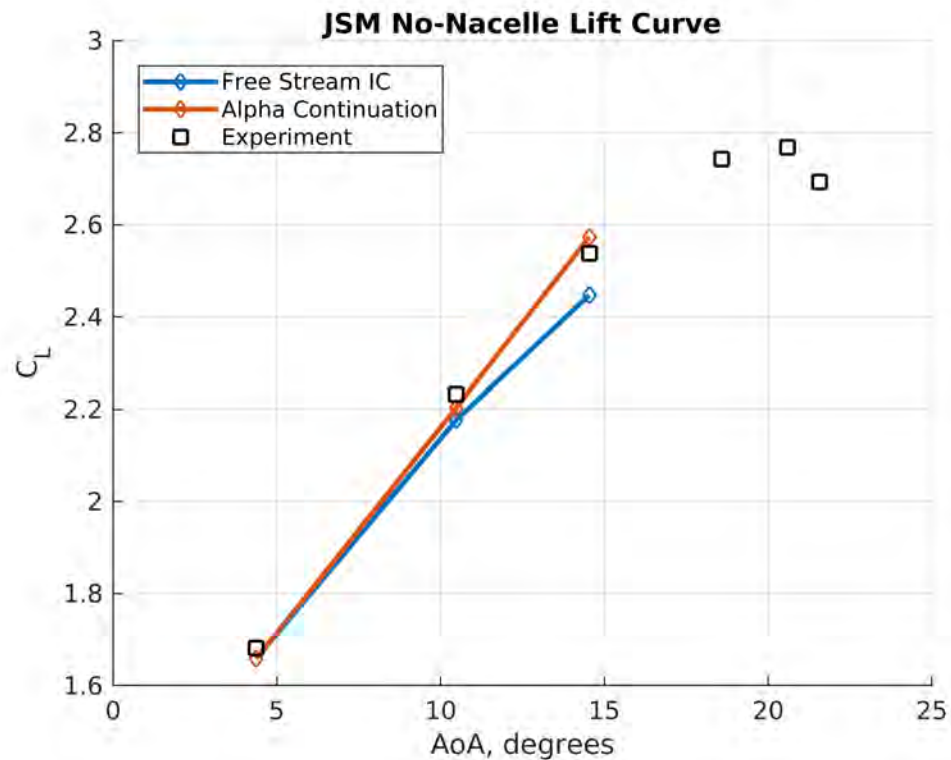


RANS computations on the JSM no-nacelle model from 3rd AIAA High-Lift Workshop¹

JSM – Effects of Initial Conditions

Linear Section of the Lift Curve

- Multiple solutions for the same AoA
- Free stream IC leads to under-prediction of lift
- Alpha continuation results match experimental lift well



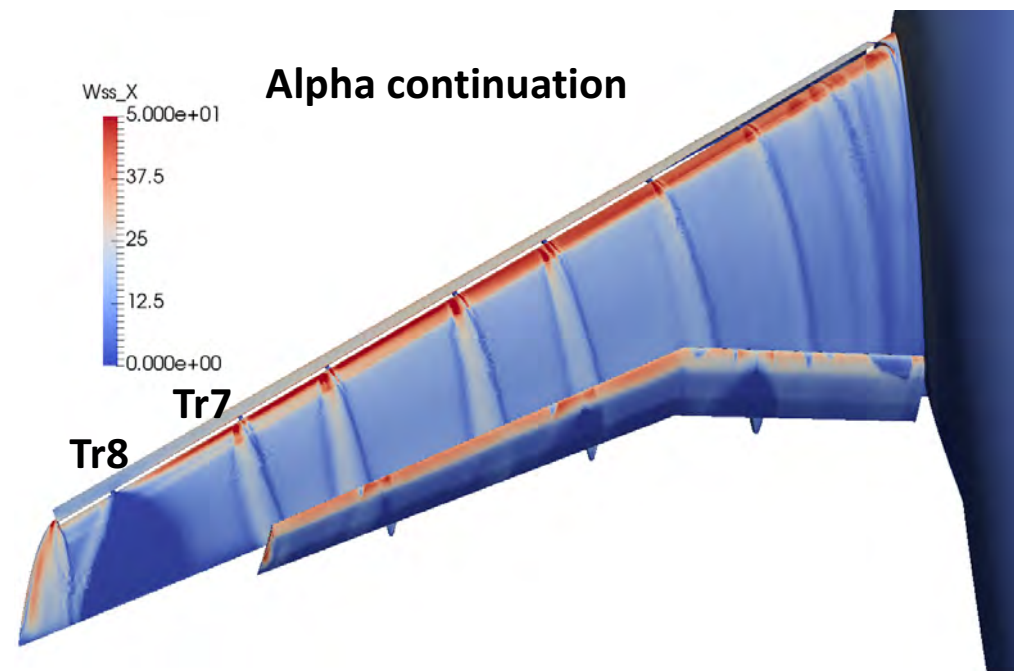
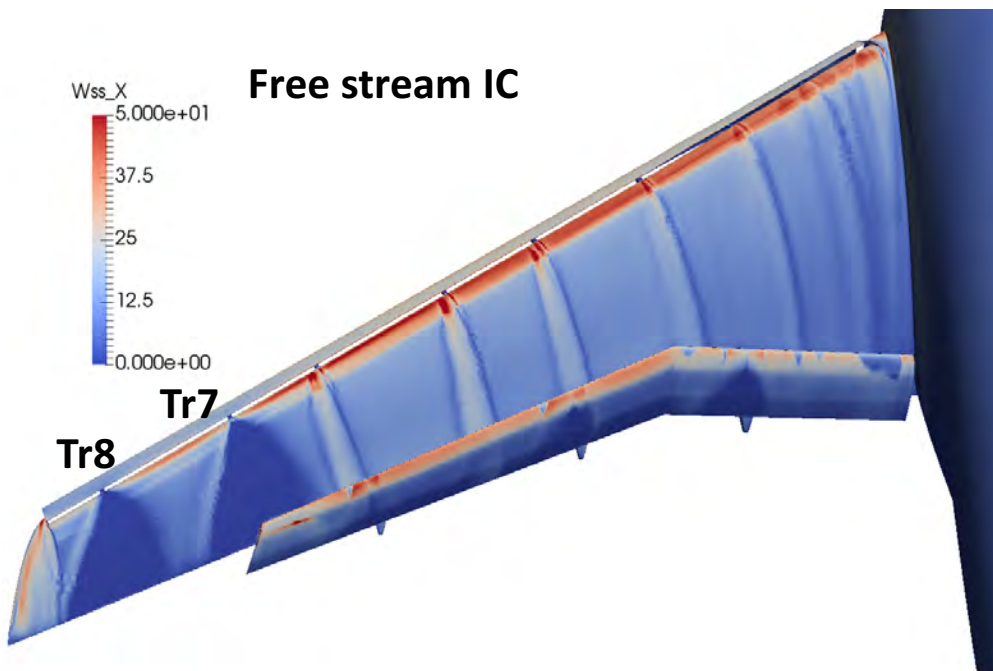
Lift coefficient vs. angle of attack (AoA)



JSM – Effects of Initial Conditions

Linear Section of the Lift Curve – 14.54° AoA

- Free stream IC shows massive separation downstream of tracks 7 and 8
- Alpha continuation solution only separated downstream of track 8, agreeing with experimental data

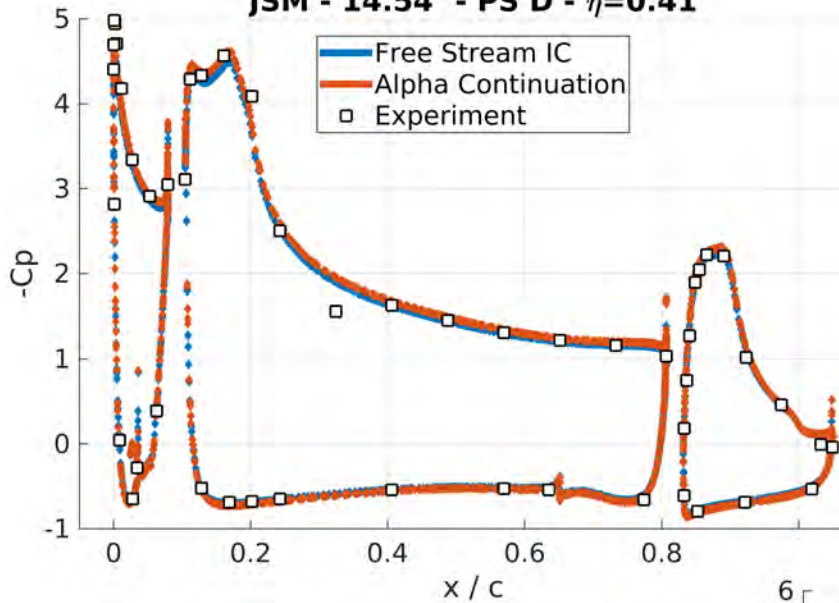


Time-averaged wall shear stress along the stream-wise direction (Wss_X)

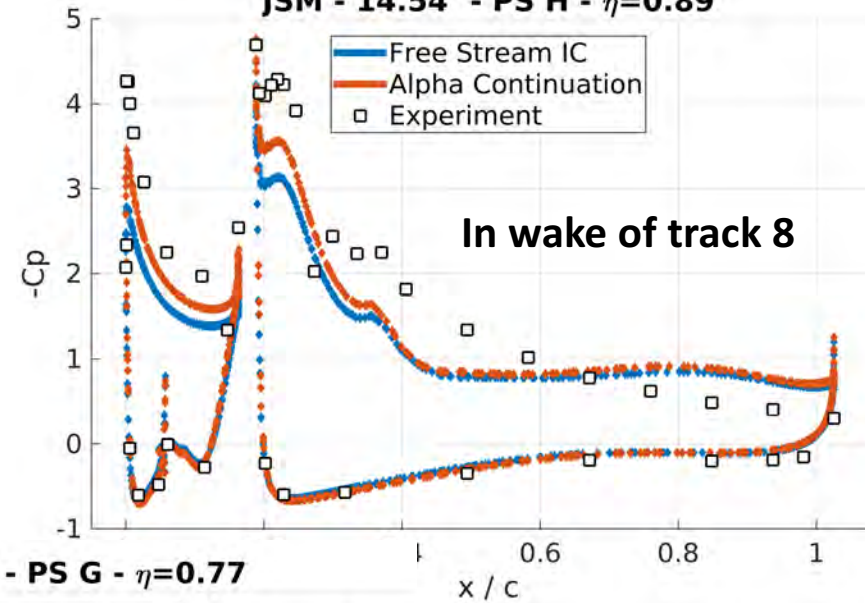


JSM – Effects of Initial Conditions

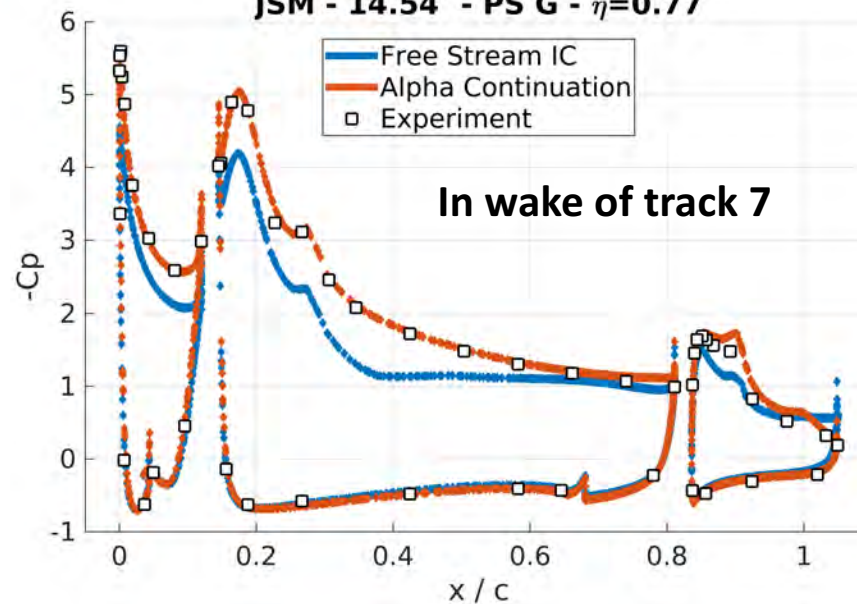
JSM - 14.54° - PS D - $\eta=0.41$



JSM - 14.54° - PS H - $\eta=0.89$



JSM - 14.54° - PS G - $\eta=0.77$



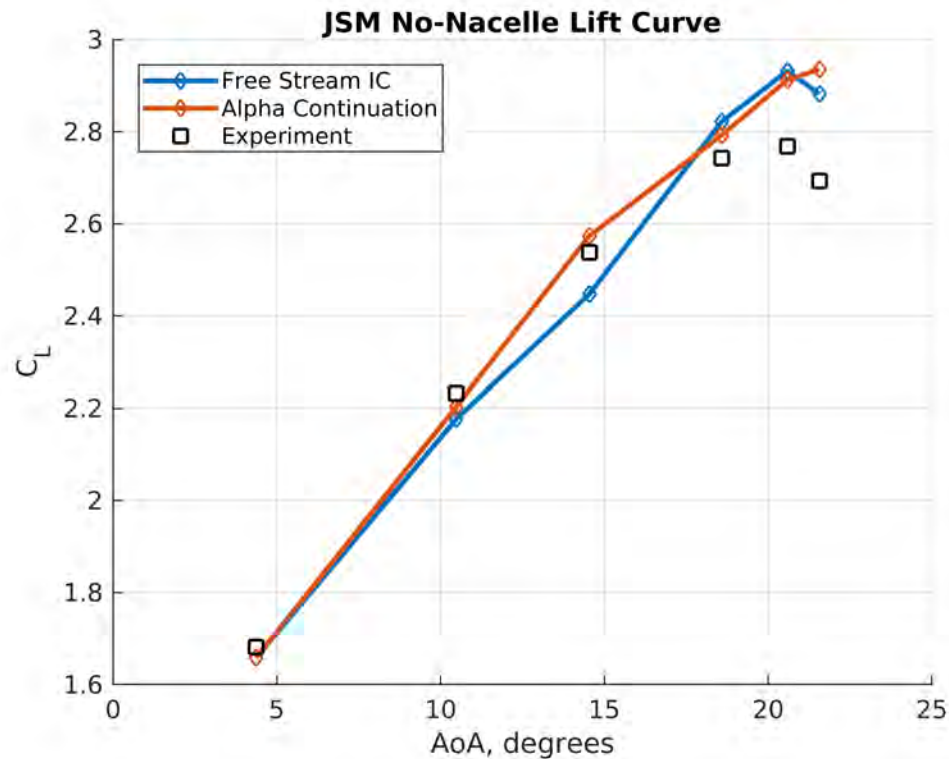
Linear Section of the
Lift Curve – 14.54° AoA



JSM – Effects of Initial Conditions

Maximum lift and stall

- Multiple solutions for the same AoA
- Both approaches over-predict maximum lift significantly
- Stall only predicted with free stream IC

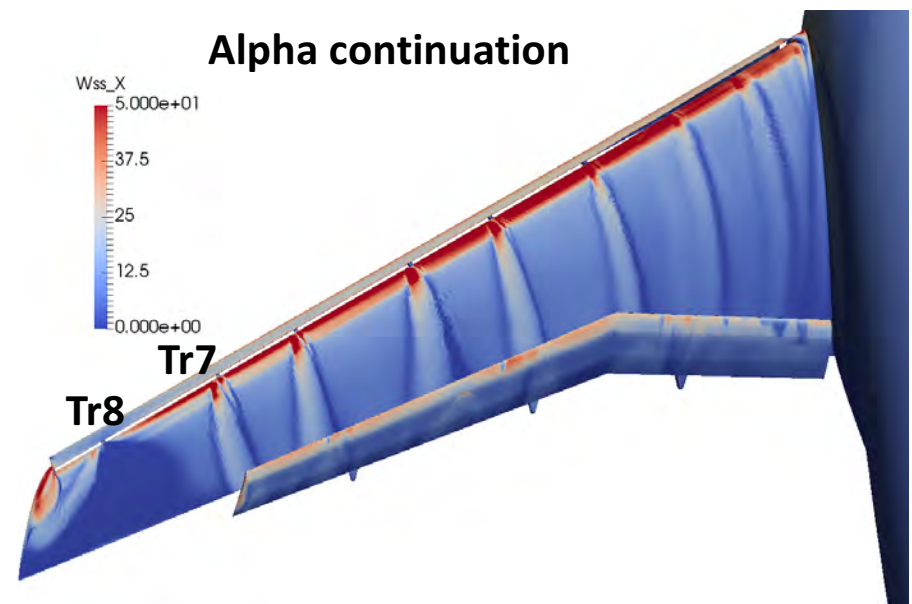
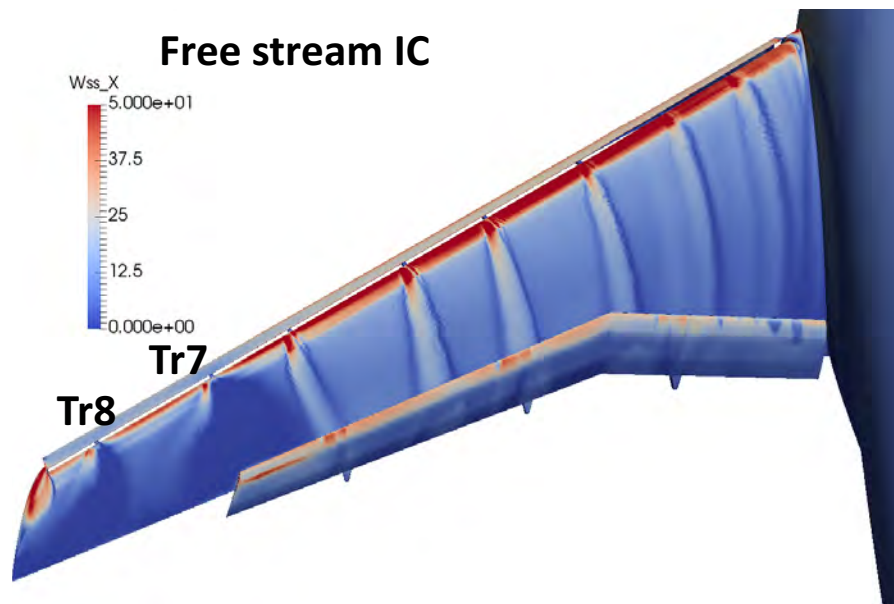
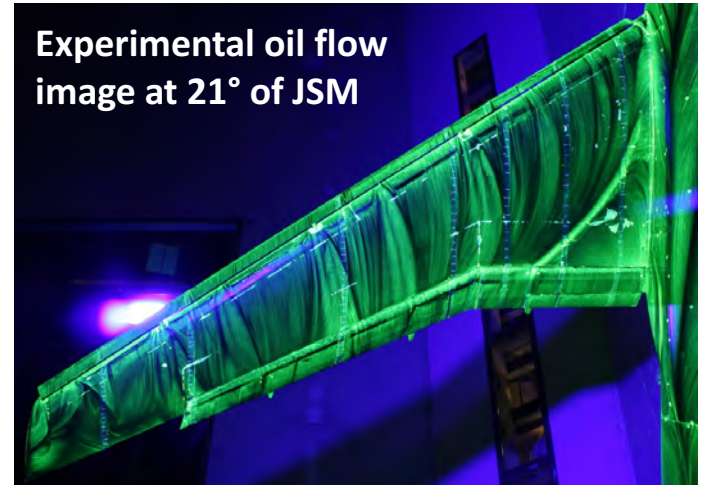


Lift coefficient vs. angle of attack (AoA)



JSM – Effects of Initial Conditions

- Both solutions miss root separation seen in experiment, over-predicting lift
- Using free stream IC leads to separation at track 7, better agreement in lift for wrong reason, wrong stall mechanism



Time-averaged wall shear stress along the stream-wise direction (Wss_X)



JSM – Effects of Initial Conditions

Interim summary:

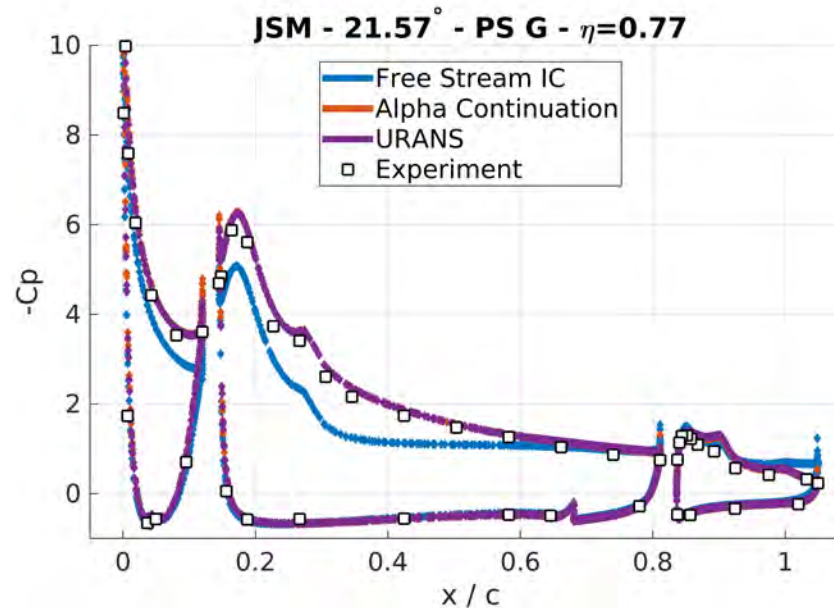
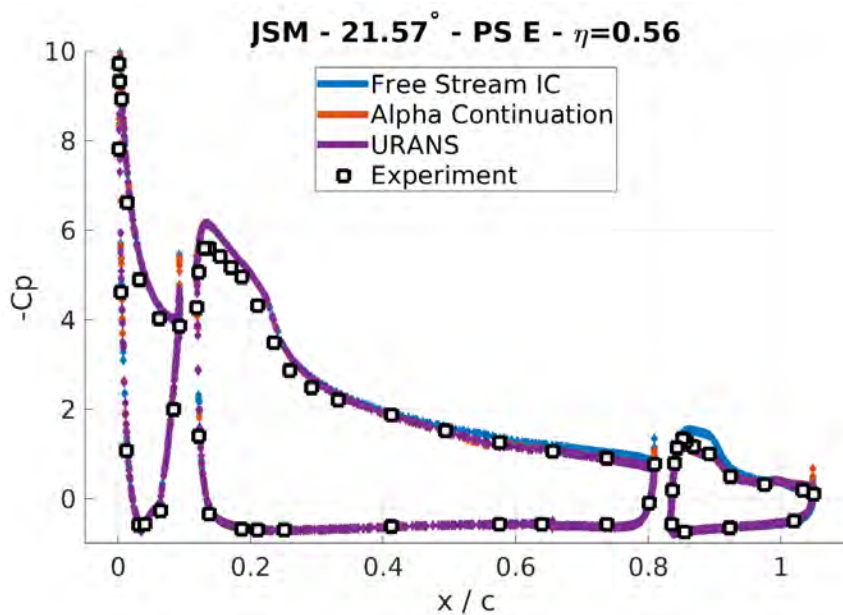
- Multiple solutions exist for the same AoA depending on ICs
- Alpha continuation approach provides improved flow field solutions
- Alpha continuation is particularly effective in linear part of the lift curve
- Free stream initial conditions can lead to overly separated flow

- Alpha continuation can be computationally expensive, requires multiple computations
- Can we converge to the high lift solution if the transient phase is not neglected with steady RANS, and instead we perform a URANS from free stream IC?

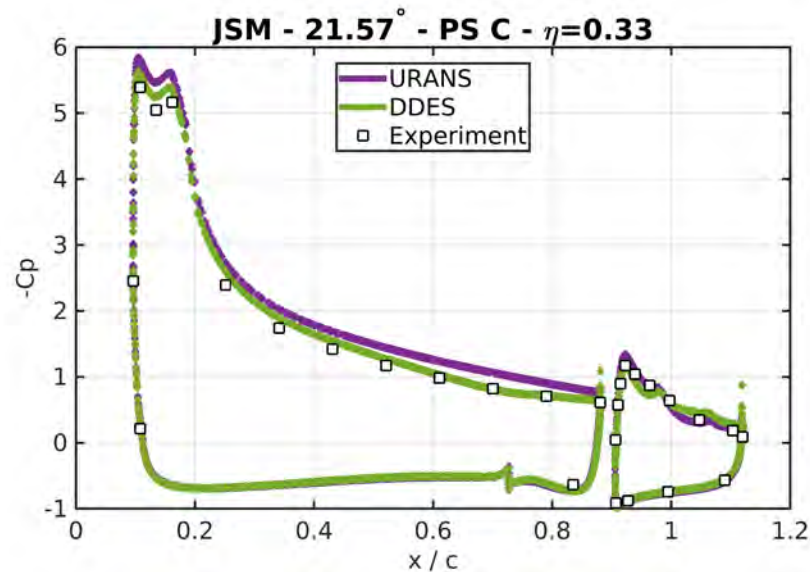
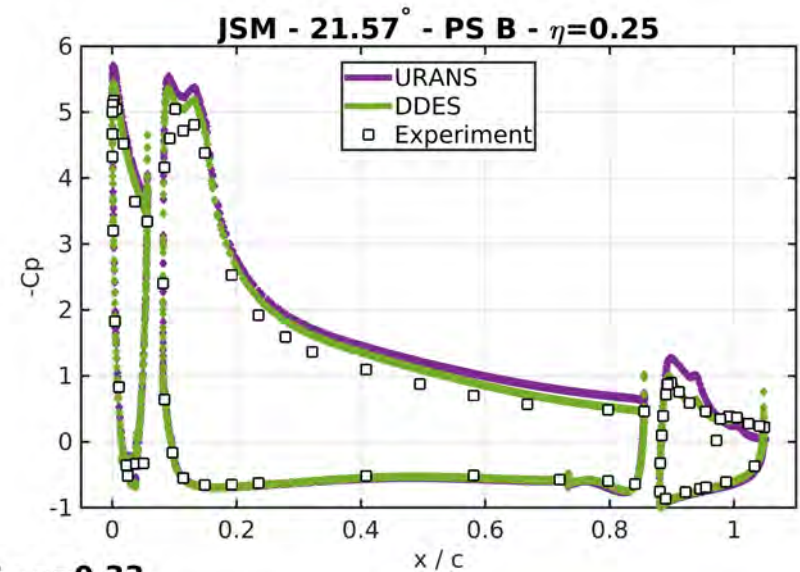
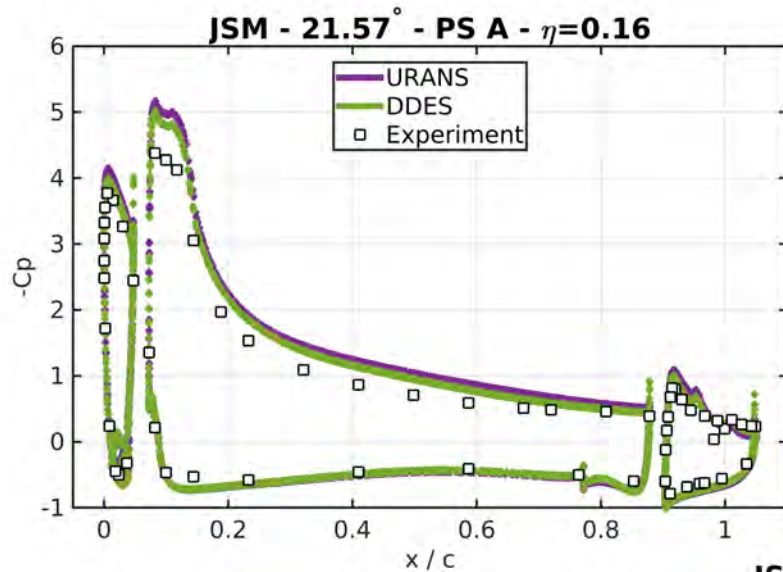


JSM – Unsteady RANS

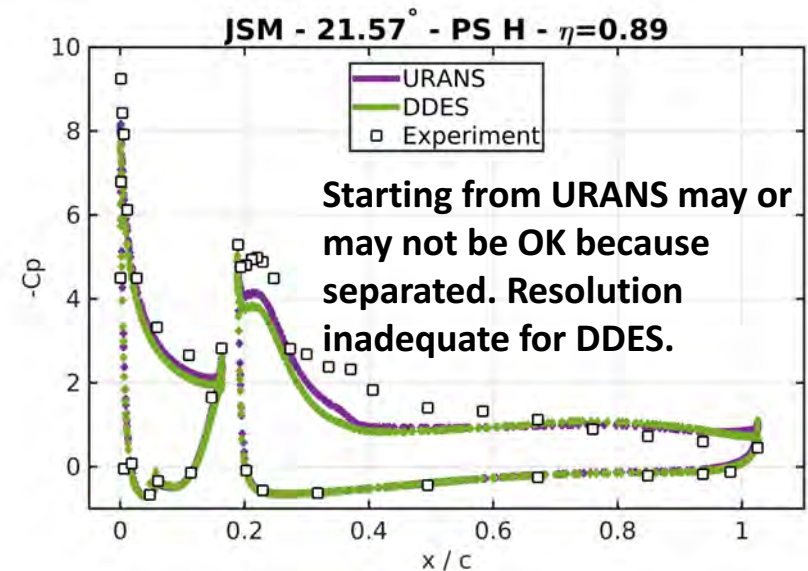
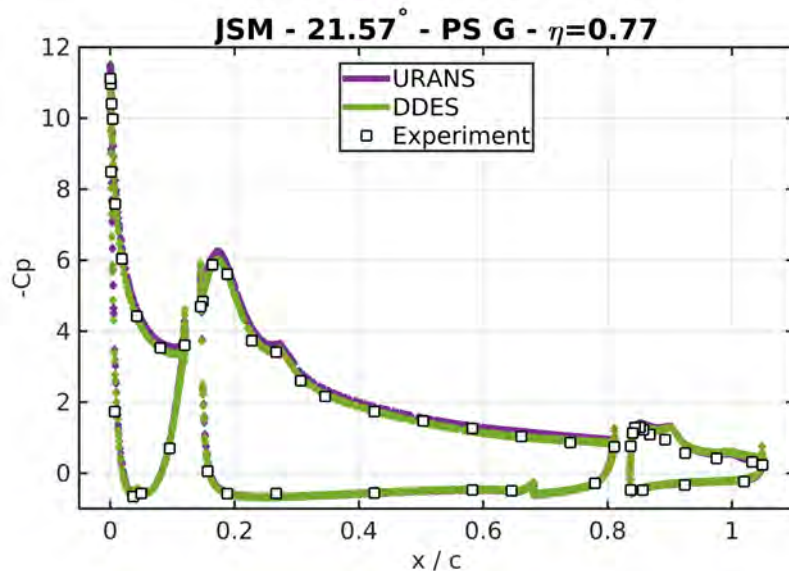
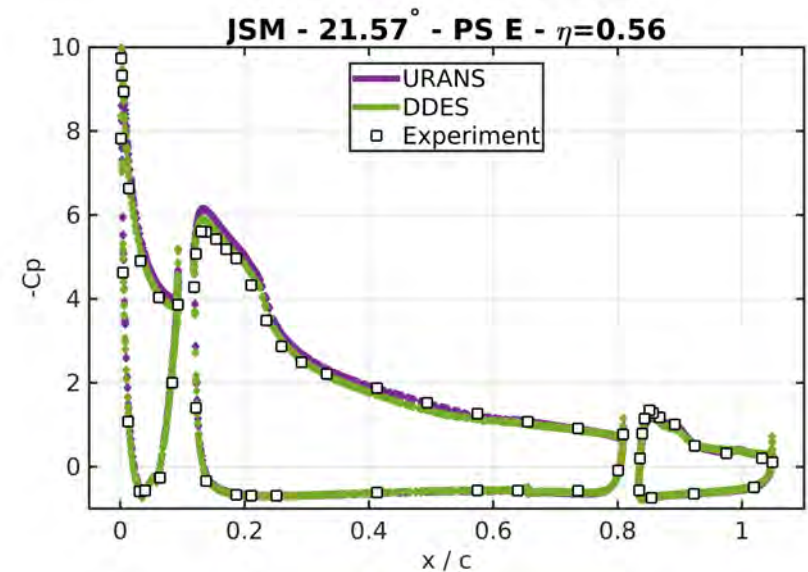
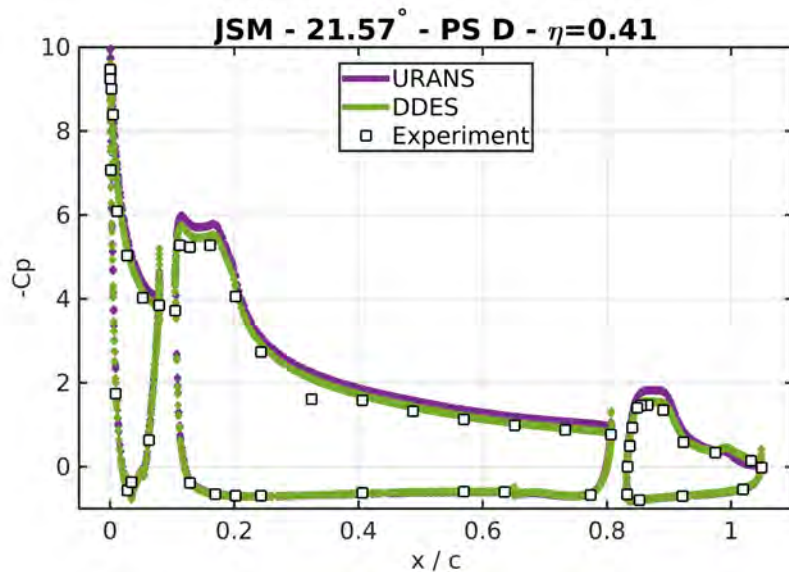
- URANS from free stream IC at 21.57° AoA
- $\Delta t_f = \Delta t c_{ref} / U_\infty = 0.05$ and $\Delta t_f = 0.01$
- time independent solution achieved with $\Delta t_f = 0.05$
- URANS achieves same solution as steady RANS with alpha continuation, for fraction of cost



JSM – DDES Pressure Profiles: Post-Stall



JSM – DDES Pressure Profiles: Post-Stall



Conclusion

- JSM: Multiple solutions exist for the same AoA depending on ICs
- Alpha continuation approach agrees well with experiments performed similarly
- RANS from free stream initial conditions can lead to overly separated flow
- URANS achieves same results as alpha-continuation with substantially less cost (for a single angle of interest).
- Preliminary DDES perform slightly better than URANS but more refinement needed
- So far DDES is not showing root stall as seen in experiments
- Will it need better transition model to capture this effect?
- HL CRM: coarse grid shows excessive separation but medium and fine in good agreement.
- Adaptive grids being pursued to understand if coarse grid + adaptivity can get fine grid quality at less than medium grid cost.
- Semi-automatic adaptivity that preserves surface grid anisotropy is showing promise to reduce number of adaptation cycles.



Acknowledgements

An award of computer time was provided by the Innovative and Novel Computational Impact on Theory and Experiment (INCITE) program. This research used resources of the **Argonne Leadership Computing Facility**, which is a DOE Office of Science User Facility supported under Contract DE-AC02-06CH11357. Specifically, the production runs were done on Mira and Cetus while the post-processing was done on Cooley.

This work also utilized the **Janus** supercomputer, which is supported by the **National Science Foundation** (award number CNS-0821794) and the **University of Colorado Boulder**. The Janus supercomputer is a joint effort of the University of Colorado Boulder, the University of Colorado Denver and the National Center for Atmospheric Research. Specifically, these resources were used in mesh generation and pre-processing.

Finally, we are grateful to acknowledge Simmetrix Inc. for their meshing and geometric modeling libraries, Acusim Software Inc. (acquired by Altair Engineering) for their linear algebra solver library, and Kitware (ParaView) for their visualization tools. The SCOREC-core mesh partitioning and adaptation tools used in this research were supported by the U.S. Department of Energy, Office of Science, Office of Advanced Scientific Computing Research, under award DE-SC00066117 (FASTMath SciDAC Institute).



Questions



References

¹J. Slotnick, T. Wayman, D. Simpson, and S. Fowler, “HiLiftPW-3: Case 2 Results.”
https://hiliftpw.larc.nasa.gov/Workshop3/HiLiftPW3-Presentations/Summary_Case2.pdf.

